AIAA AVIATION Forum
5-9 June 2017, Denver, Colorado
17th AIAA Aviation Technology, Integration, and Operations Conference
10.2514/6.2017-3266

The Doghouse Plot: History, Construction Techniques, and Application

John R. Wilson[1]
Arizona State University, Tempe, AZ, 85283

and

Timothy T. Takahashi[2]
Arizona State University, Tempe, AZ, 85283

The Doghouse plot visually represents an aircraft's performance during combined turn-climb maneuvers. The Doghouse plot completely describes the turn-climb capability of an aircraft; a single plot demonstrates the relationship between climb performance, turn rate, turn radius, stall margin, and bank angle. Using NASA legacy codes, EDET and NPSS, we can reverse engineer sufficient basis data for commercial and military aircraft to construct Doghouse plots. Engineers and operators can then use these to assess their aircraft's full performance envelope. The insight gained from these plots can broaden the understanding of an aircraft's performance and, in turn, broaden the operational scope of some aircraft that would otherwise be limited by the simplifications found in their Airplane Flight Manuals. More importantly, these plots can build on the current standards of obstacle avoidance and expose risks in operation.

Nomenclature

a_c	=	centripetal acceleration
AEO	=	all engines operating
AFM	=	aircraft flight manual
ALT	=	altitude
C_D	=	drag coefficient
C_L	=	lift coefficient
D	=	drag force
g	=	gravitational acceleration
IAS	=	indicated airspeed
K_{accel}	=	rate-of-climb correction factor
L	=	lift force
M	=	Mach number
$N1_{max}$	=	maximum shaft rotation speed
N_z	=	load factor
OEI	=	one engine inoperative
R	=	turn radius
S_{ref}	=	reference area
SSR	=	stall speed ratio
T	=	thrust
TAS	=	true airspeed
TSFC	=	thrust specific fuel consumption

[1] M.S. Candidate and Research Assistant, School of Engineering of Matter Transportation & Energy, P.O. Box 876106, Tempe, AZ, and AIAA Student Member.

[2] Professor of Practice, Aerospace and Mechanical Engineering, School of Engineering of Matter, Transport & Energy, P.O. Box 876106, Tempe, AZ, and Associate Fellow AIAA.

V_A = design maneuvering airspeed
V_C = cruise speed
V_G = ground speed
V_{KTAS} = true airspeed (knots)
V_{SR} = reference stall speed
V_{SR0} = reference stall speed in landing configuration
V_W = wind speed
W = instantaneous flight weight
Φ = bank angle
θ = oncoming wind angle

I. Introduction

ENERGY-MANUEVERABILITY theory was developed in the early 1960's by fighter pilot turned aeronautical engineer John Boyd. The theory exploits a pilot's capability to command the exchange of potential and kinetic energy, while also considering the aircraft's capacity to gain energy. The "Mad Major" Boyd and cohort Thomas Christie developed E-M theory as an unauthorized project during their time in the Air Force.[1] Boyd believed that his theory would enable America to dominate air combat. The initial motivation of E-M theory was to "understand the full performance envelope of American aircraft, with the goal of developing new tactics for aerial battles."[1] Boyd was interested in a pilot's capability to gain energy at a specific altitude, load factor (i.e. turn rate) and speed. He also wanted his theory to be blind to the differences of various aircraft, it was to be normalized and therefore independent of weight.

Boyd later realized that, with E-M theory, he could reverse engineer enemy aircraft. He could understand their performance capabilities possibly even better than their creators did. Boyd would eventually go on to play a significant role in developing the F-15 and F-16 combat aircraft using E-M charts as a primary argument for his design choices.[1]

Assessing an aircraft's performance is analyzing the entire aircraft and every facet of its operation. For combat maneuvering and fighter tactics, climb, turn, and acceleration are the critical aspects of flight performance. Other flight characteristics such as takeoff, landing, and range are merely factors of how the aircraft arrives at its intended environment.

Ultimately, climb, turn, and acceleration characteristics dictate how an aircraft will perform as a fighter.[2] In his original treatise, Boyd presented two styles of plots to study the maneuverability of an aircraft. Instantaneous maneuverability is shown in plots that vary as load factor versus velocity. In an instantaneous maneuver, the aircraft is expected to change speed and altitude as a result of a sudden pilot command. In addition, Boyd became interested in understanding sustained maneuverability in which the aircraft does not change speed nor altitude as a result of its turn. Representations of sustained turning maneuvers were visualized through energy contours plots upon a Mach number versus altitude grid.

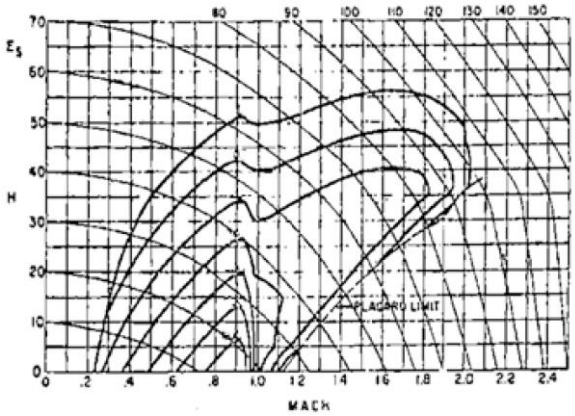

Figure 1. F-4C Maximum Power 1-G Energy Rate Diagram. *Boyd uses this plot to compare the maneuvering capabilities of the F-4C Phantom to the Soviet MiG-21.*

Boyd realized that all maneuvering, sustained or instantaneous, must be conducted between an energy state at the initial altitude-airspeed and a minimum energy state at zero altitude and minimum airspeed. In air-to-air combat, maneuvering advantage is given to the pilot who can either enter an offensive engagement at a higher initial energy level or has the capability to gain more energy during the course of the battle. Figure 1 is a visualization of the F-4C Phantom's 1-G Energy Rate and was used to illustrate its capabilities against the Soviet MiG-21. With such plots, fighter aircraft design was elevated.[3]

The Doghouse plot presented in this paper is an improved version of the E-M diagrams presented by Boyd. We present a hypothetical Doghouse plot in Figure 2 as an example. The Doghouse plot is a composition of many flight characteristics and can seem cluttered at first glance. However, the Doghouse plot gives a massive amount of information of an aircraft's performance during a turn in a useful way. The horizontal axis is given as the true airspeed, in knots, (V_{KTAS}) while the vertical axis is the turn rate, or rate of heading change, given in degrees per second. To visualize climb performance, a colored contour of climb gradient is plotted for every combination of airspeed and turn rate. Lines of constant turn radius, stall speed ratio (*SSR*), and bank angle are superimposed onto of the climb gradient to define the turn and stall margin. These lines of constants completely define the turning maneuver while the climb gradient shows the associated climb performance. The idea is to show how aggressively an aircraft can turn and while maintaining a desirable climb gradient.

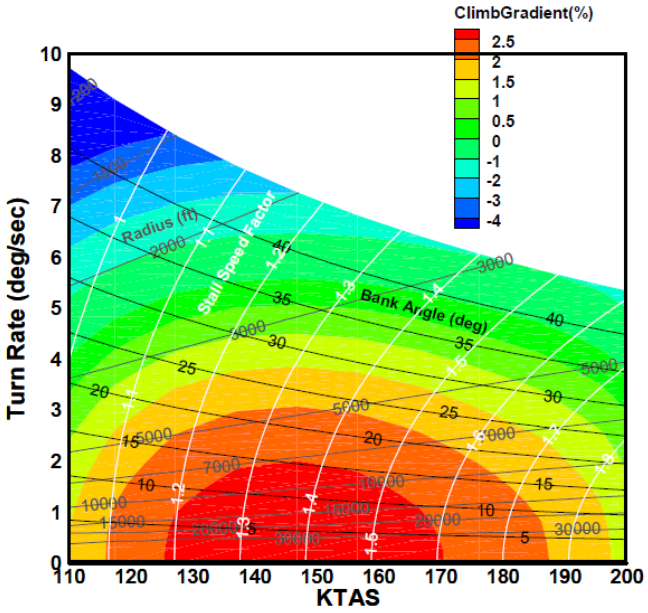

Figure 2. Hypothetical Doghouse plot. *This figure is a doghouse plot. Moving vertically from a given TAS shows the turning and climb performance in the same plot.*

The benefit of the Doghouse plot transcends fighter aircraft design. There is a clear benefit for producing Doghouse plots for civilian transport aircraft. While transport aircraft are not designed solely to maximize maneuverability and climb performance, the insight gained from the Doghouse plot can be used to design superior aircraft and expand operation of aircraft currently in service.

Federal regulations require that an aircraft must maintain a certain level of climb performance in all-engines-operating (AEO) and one-engine-inoperative (OEI) scenarios.[4,5] These requirements for climb performance directly affect the takeoff procedure of an aircraft. In a climb that requires a turn to avoid either an obstacle or a restricted airspace, the obtainable climb gradient while turning must be understood to ensure safety. All civilian operators must plan for these critical OEI scenarios.[6] If an aircraft must turn to avoid an obstacle and there is insufficient climb performance to successfully perform the avoidance maneuver, the aircraft will either collide with the obstacle or run the risk of stalling and falling out of the sky. Both scenarios are incredibly undesirable. In order to avoid controlled flight into terrain pilots, dispatch, and airframe manufactures, need to understand an aircraft's performance throughout a sustained turn-climb.

Under current FAA rules, an aircraft is not allowed to takeoff if it does not meet a certain minimum climb performance or net climb performance.[7,8] Weight at takeoff (*WAT*) limits guarantee dispatch weight does not exceed minimum climb gradients at liftoff, second segment (take-off flaps, gear up), final segment (cruise flaps, gear up) under engine inoperative situations. Second and final segment climb gradient charts support the construction of minimum altitude vs downrange distance charts to ensure sufficient obstacle clearance during climb out. These charts are reported as "net climb" gradients – which have a federally regulated performance demerit applied to them.[9] The reduced reported performance grants some extra margin for climb degradation that arises from maneuvering and from unexpected tailwinds during climb out.

The OEI takeoff flight path must guarantee that the aircraft clears all obstacles by 35 feet vertically, or by 200 feet horizontally within airport limits, and 300 feet outside of airport limits.[7] Aircraft at higher weights can be susceptible to disqualification due to climb performance requirements. An overweight aircraft must unload fuel or payload in order meet climb requirements.

When dispatch plans a flight, it is important that they truly understand an aircraft's capability of retaining a climb gradient while executing a turn. Consider a flight from an airport located in a valley; KBUR (Burbank) is an excellent example. Refer to Figures 3 and 4 to see the close proximity of mountainous terrain to the end of the primary runway.[10] To fly the most popular standard instrument departure (SID) for Burbank, the Van Nuys 3 departure[11] (see Figure 5), the pilot must turn from the runway compass heading of 335º to a heading of 255º shortly after liftoff. Thus, the SID requires the pilot to make this 80º heading change to the left all while maintaining a minimum climb gradient of 550-ft per nautical mile until the aircraft reaches 5000-ft pressure altitude (this implies an ~9% climb gradient including a sharp turn). If the aircraft cannot maintain a 9% climb gradient (very likely when flying an aircraft with poor engine inoperative climb performance such as a Canadair CRJ-200), it becomes trapped in the valley and must abandon its scheduled flight path to seek an emergency landing.

It is not easy for a pilot or dispatch engineer to plan these common departures. The FAA requires that operators must include basic OEI climb performance charts in the AFM. These charts need to account for variations in weight and airport conditions, such as altitude and temperature as well as headwind/tailwinds.[12] This data is crucial, but it alone does not provide a deep understanding of the total maneuvering envelope of the aircraft.

Flights will dispatch based upon limited OEI performance information. For example, the manufacturer need not document the climb performance degradation associated with a turn. In addition, a 90º heading change during initial climb out will probably null the beneficial effects of prevailing headwinds. Circling in an attempt to gain altitude is likely to result in the aircraft flying in a tailwind situation (one that further reduces the effective climb gradient).

Ideally, both dispatch and pilots should know how an aircraft performs in climb as a function of weight, altitude, temperature, flight speed, wind speed, and bank angle. This expansion of climb data would allow dispatch to better plan for climb outs that require turns for obstacle avoidance. This nuanced understanding of an aircraft would lead to better quality dispatch which, when associated with higher dispatch weights, can reduce the need for refueling stops, stranded passengers, or misconnected luggage. Both the operator and the consumer would benefit from this knowledge.

Figure 3. View from end of runway 33 at KBUR. *Picture taken facing north.*

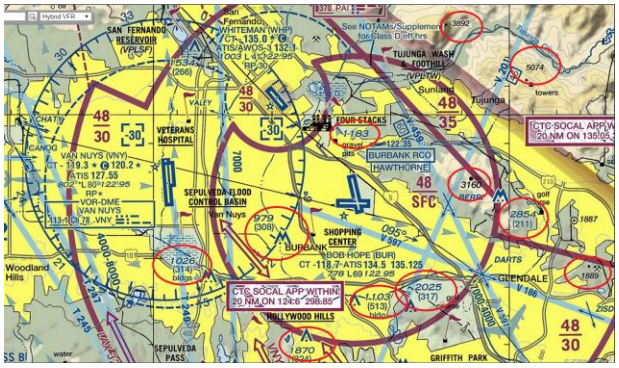

Figure 4. VFR chart for Burbank (KBUR) Airport.[10]

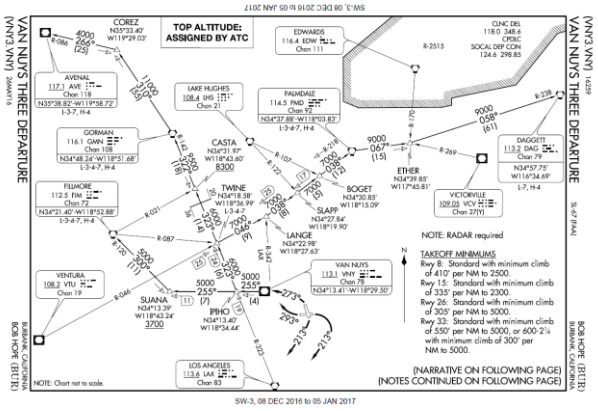

Figure 5. Van Nuys Three Standard Instrument Departure from Burbank Airport (KBUR).[11]

Although the Doghouse plot is not found in typical commercial airplane AFMs, it can be used to expand the operational capabilities of aircraft currently in service. Better informed pilots and dispatchers can make better informed decisions. For aircraft that are already in service, rewriting the FAA approved AFM is out of the question since it would need to be certified under a separate supplement type-certificate. Nonetheless, it is possible to reverse engineer these aircraft in order to expand understanding of their true flight characteristics.

With proper aircraft data to model drag and propulsion, Doghouse plots can be assembled a posteriori initial aircraft certification. With the Doghouse plot, flight simulators tests can verify data produced in this study and test takeoff paths that are currently restricted for certain aircraft and airports. The insight gained from the Doghouse plot will also allow for improved dispatching of cue speeds thereby maximizing climb out performance and efficiency.

For many aircraft, the AFM is compiled to meet the minimum requirements for certification. Although certification ensures reasonably safe operation of an aircraft, robust understanding of the aircraft's performance is undocumented. At one level, it is reasonable not to bombard a pilot with superfluous information, but to accept the performance and operational guidelines within the AFM as dogma may comprise performance.

An aircraft can show capability beyond what is documented in the AFM in many cases. Some transport category AFMs examined in this study include large sections of, "non-FAA approved" performance charts that cover scenarios that are not required by the FAA.[13] Generally, the insight in these charts are of immense value. However, the FAA is not culpable if these numbers are wrong or misleading in any way. The burden falls on the manufacturers to produce quality data that expands beyond the FAA requirements. Ideally, the manufacturer would provide all data possible to ensure the utmost safety and the most comprehensive understanding of their aircraft. Unfortunately, this is not the case. Aircraft with AFMs constructed to only meet or barely exceed FAA minimums are likely not being used to their absolute potential. FAA minimums ensure safe operation and some level operational capacity; however, it is likely that the operational scope of these aircraft can be magnified.

The Doghouse plot would fall into the category of, "non-FAA approved" performance charts, but would aid in proving compliance with FAA required climb performance and operating procedures. The net takeoff flight path is meant to encompass all factors that would degrade climb performance since the minimum climb requirement does not include factors like banking, wind disturbances, and suboptimal engine performance. Oddly, in order to comply with the FAA requirements for obstacle clearance flight path analysis, AFMs should include figures such as the Doghouse plot which are neither required, nor approved, by the FAA for type certificate compliance.

There is a disconnect between engineers' design goals and pilot's "stick-and-rudder" feel of aircraft performance. This is partly due to the complexity and ambiguity of AFMs. The derivations and the assumptions for certain given values within the AFM do not provide the flight crew enough understanding of their craft and can then limit performance. Pilots use best practices that are not defended by actual data, but rather are learned through flying. A better practice would be to study credible data models of aircraft performance and then alter execution in order to achieve a truly optimal maneuver. In order to do this there must first be actual data to train pilots. For transport category aircraft, the Doghouse plot can help engineers develop improved piloting practices that enhance climb performance and safety.

Credible models for maneuvers that require combined turning and climbing are formulated in this paper. The regulatory framework which inspire the creation of this data is covered in the next section. Then, underlying equations for a turning maneuver and climb are developed. Using general purpose aerodynamic and propulsive analysis tools, data of a reverse engineered aircraft can be formulated in Excel VBA. With this data, Doghouse plots can be assembled for any aircraft using basic dimensions and understanding of its powerplant. Once the doghouse is formulated, better strategies for dispatching can be made. Knowing the climb, takeoff, and obstacle avoidance requirements for a given mission the optimal cue speed for an aircraft can be found to optimize the safety and efficiency of a mission.

II. Regulatory Framework Applicable to Turn-Climbs & Obstacle Avoidance

The Code of Federal Regulations (CFR) defines the operating procedures and requirements of any transport category aircraft. Four categories of regulations are pertinent to the construction and implementation of the Doghouse plot and are covered in this section. First are the regulations that define climb gradient and takeoff path requirements. Second, the group of regulations that define the different cue speeds. Third, the regulations that cover what is required in an AFM for type certification. Last is the advisement set forth by the FAA in AC-120-91 in the scope of obstacle avoidance.

A. Climb Gradient and Takeoff Path Regulations

Title 14 CFR Part 25 controls the acceptable climb gradients for an aircraft:

14 CFR § 25.111 – Takeoff path defines the takeoff path as the point of standing start to the point at which the aircraft is 1,500 ft. above the takeoff surface, or the point at which the aircraft transitions to its enroute configuration and V_{FTO} is reached. It also states that at each point in the takeoff path from standing start to 400 ft. above the takeoff surface, the aircraft must have an available climb gradient of 1.2% for two-engine airplanes, 1.5% for three-engine airplanes, and 1.7% for four-engine airplanes. It states that the configuration may not be changed except for landing gear retraction of propeller feathering in compliance with this regulation.[14]

14 CFR § 25.115 – Takeoff flight path states that the net takeoff flight path data must be determined so that they represent the actual takeoff flight paths reduced at each point by a gradient of climb equal to: 0.8% for two-engine airplanes, 0.9% for three-engine airplanes, and 1.0% for four-engine airplanes. The prescribed reduction in climb gradient may be applied as an equivalent reduction in acceleration along the part of the takeoff flight path at which the airplane is accelerated in level flight.[15]

14 CFR § 25.121 – Climb: One-engine-inoperative defines the minimum climb performance of an aircraft with a critical engine failure in takeoff and enroute configurations. In the takeoff configuration with the landing gear extended, the steady gradient of climb must positive for a two-engine aircraft, 0.3% for a three-engine airplane, and 0.5% for a four-engine airplane. In takeoff configuration with the landing gear retracted the steady climb gradient may not be less than 2.4% for two engine airplanes, 2.7% for three engine airplanes, and 3.0% for four engine airplanes. In the final takeoff, or enroute configuration the steady gradient of climb may not be less than 1.2% for two-engine airplane, 1.5% for three-engine airplanes, and 1.7% for four-engine airplanes. In the approach configuration, the aircraft must maintain a steady climb gradient of 2.1% for two-engine airplanes, 2.4% for three-engine airplanes, and 2.7% for four-engine airplanes. The approach configuration includes a critical inoperative engine, is at maximum landing weight, and has the landing gear retracted.[5]

14 CFR § 25.123 – Enroute flight paths require that flight paths in an enroute configuration must be determined at each weight, altitude, and ambient temperature within the operating limits established for the airplane. The minimum speed in the enroute configuration is the final takeoff speed, V_{FTO}. In OEI, icing, and non-icing conditions, paragraph (b) of this regulation states that the flight path data must represent the actual climb performance diminished by a gradient of climb of 1.1% for two-engine airplane, 1.4% for three-engine airplanes, and 1.6% for four-engine airplanes.[8]

14 CFR § 25.119 – Landing climb: All-engines-operating states that, "the steady climb gradient for an aircraft in landing configuration must not be less than 3.2%, with the engines at the power or thrust that is available 8 seconds after initiation of movement of the power or thrust controls from minimum flight idle to the go-around power or thrust setting."[16] If an engine fails during a balked landing, pilots need to reconfigure their aircraft into the second segment climb configuration as soon as possible in order to climb out at V_2, the takeoff obstacle clearance speed.

It is clearly defined that an aircraft must maintain a certain climb gradient for AEO and OEI conditions. The CFR does not specifically distinguish from takeoff paths that also require turns. At some airfields, it is unavoidable to fly a purely straight route, making the true requirement for climb out unclear based on CFR regulations alone. The degradation in acceptable climb gradients in 14 CFR § 25.115 aims to encompass all detrimental effects such as wind, engine health and turning. By prescribing an overall decrease of the actual climb performance, the FAA aims to take a more pessimistic view of what the actual climb gradient will be in actual operation. While this does form

some level of safety, understanding of the true performance of an aircraft is not explicitly required. It is only assumed that the loss is climbing capabilities will fall within the degradations defined in 14 CFR § 25.115. This loss in climb gradient is not specifically investigated in the AFM and for many aircraft these losses are not properly modeled.

14 CFR Parts 121 & 135 regulate the operation of a transport category aircraft and smaller commuter aircraft. The regulations that control the limitations of takeoff in respect to obstacle clearance are identical.

14 CFR § 121.189 – "Airplanes: Turbine engine powered: Takeoff limitations" and 14 CFR §135.379 "Large transport category airplanes: Turbine engine powered: Takeoff limitations" give two sets of required clearance distances in respect to the certification date of the aircraft. The regulations state that,

> "(d) No person operating a turbine engine powered large transport category airplane may take off that airplane at a weight greater than that listed in the Airplane Flight Manual— (1) For an airplane certificated after August 26, 1957, but before October 1, 1958 (SR422), that allows a takeoff path that clears all obstacles either by at least (35 + 0.01 D) feet vertically (D is the distance along the intended flight path from the end of the runway in feet), or by at least 200 feet horizontally within the airport boundaries and by at least 300 feet horizontally after passing the boundaries; or (2) For an airplane certificated after September 30, 1958 (SR422A, 422B), that allows a net takeoff flight path that clears all obstacles either by a height of at least 35 feet vertically, or by at least 200 feet horizontally within the airport boundaries and by at least 300 feet horizontally after passing the boundaries. (f) For the purposes of this section, it is assumed that the airplane is not banked before reaching a height of 50 feet, as shown by the takeoff path or net takeoff flight path data (as appropriate) in the Airplane Flight Manual, and after that the maximum bank is not more than 15 degrees."[7]

14 CFR § 135.398 – Commuter category airplanes performance operating limitations follow the later requirements of obstacle clearances of 35 feet vertically or by at least 200 feet horizontally within the airport boundaries and by at least 300 feet horizontally after passing the boundaries. It also assumes that the airplane is not banked before reaching a height of 50 feet and after the bank is not more than 15 degrees.[17]

B. Cue Speed Regulations

The insight from Doghouse plots can improve the dispatching of cue speeds. Figure 6 shows that better scheduling of cue speeds improves climbing performance and obstacle avoidance. The CFR defines many cue speeds in relation to the stall speed and minimum control speeds. Since the Doghouse plot has superimposed lines of SSR, the change in climb performance can be quickly assessed at a given cue speed for a variety of turning maneuvers.

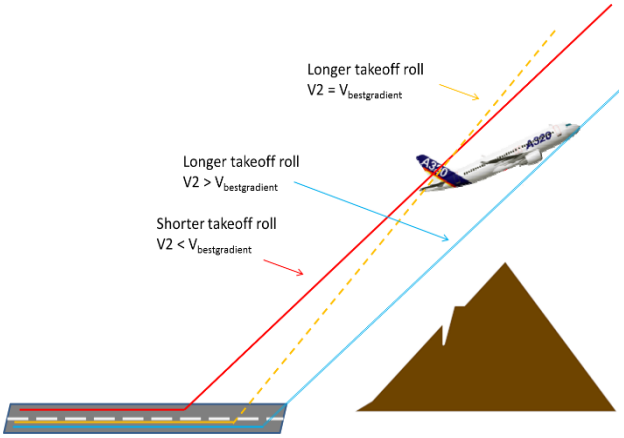

Figure 6. Optimal Cue Speed Schematic. *This figure shows the basic principle of the importance of scheduling the optimal cue speed regarding obstacle avoidance. There exists an optimal takeoff speed which will correspond to the maximum ROC.*

14 CFR § 25.107 – Takeoff speeds defines the different cueing speeds in takeoff configuration. The minimum takeoff speed is the maximum between 1.13 V_{SR} and 1.10 V_{MC}. The final takeoff speed V_{FTO} may not be less than 1.18 V_{SR} or the speed that provides the least gradient of climb required in § 25.121. This regulation also allows for the use of these cue speeds in icing and non-icing conditions.[18]

14 CFR § 25.121 – Climb: One-engine-inoperative also states that, in approach configuration, the aircraft must retain a certain climb performance with a climb speed established in connection with normal landing procedures, but not exceeding 1.40 V_{SR}. Therefore, at initial approach, the speed of the aircraft is at most the maximum between 1.40 V_{SR} and V_{MCA}. At a minimum, the stall speed in the initial approach configuration with a critical engine failure will not exceed 1.10 V_{SR} in AEO condition. At a given speed flap deflection increases SSR which reduces the maximum approach speed. The combination of large flap deflection, steep flight path angle, and low airspeed will drastically reduce climb performance if a balked landing is required.

14 CFR § 25.125 – Landing states that the refusal speed of final approach may not be less than 1.23 V_{SR0} or V_{MCL} in non-icing conditions. This regulation also requires that the horizontal landing distance must be calculated for standard temperatures for each weight, altitude, and wind within operational limits.[19]

14 CFR § 25.149 – Minimum control speed defines V_{MC} as the minimum calibrated airspeed at which the aircraft is still controllable when a critical engine fails. In OEI condition at V_{MC}, the aircraft must be able to maintain straight flight with an angle of bank not more than 5 degrees. Also, V_{MC} may not be less than 1.13 V_{SR}.[20] A combination of bank and rudder deflection can be used to optimally trim the aircraft, but the resulting attitude of the aircraft would increase drag and reduce airspeed. Both turn and climb performance would fall resulting in a low performance scenario.

14 CFR § 25.335 – Design airspeeds sets the minimum maneuvering speed V_A as $V_{S1}\sqrt{n}$, where n is the positive limit on maneuvering load factor.[21] V_A does not need to be greater than the cruise speed V_C. While V_A is not intended to be the speed that allows for unrestricted flight-control movement without exceeding airplane structural limit, it is advised against performing maneuvers near or above V_A.[22] If V_A is sufficiently high this is a nonissue in obstacle avoidance due to the 250 V_{KIAS} limit below 10,000 ft. altitude prescribed in 14 CFR § 91.117.[23]

C. Aircraft Flight Manual Requirements

The AFM section of 14 CFR Part 25 – Airworthiness Standards: Transport Category Airplanes states the type of information that must be furnished by the applicant within the AFM. These regulations require the information for safe operation of the aircraft.

14 CFR § 25.1581 – General states that the AFM must furnish information required within the AFM section of the CFR. Additionally it requires, "other information that is necessary for safe operation because of design, operating, or handling characteristics." Information required by the regulations must be also verified and approved by the FAA. Any other information that is not verified or FAA approved must be identified and segregated from the FAA-approved information.[11]

14 CFR § 25.1585 – Operating procedures requires the furnishing of operating procedures for normal or routine operation. It also requires non-normal procedures in case of malfunction or failure that require any deviation in use of regular systems. Lastly, emergency procedures that require immediate and precise action by the crew to substantially reduce the risk of catastrophe must be furnished by the applicant.[6]

14 CFR § 25.1587 – Performance information requires furnishing of the performance information computed under §25.115, §25.123, and §25.125 for the weights, altitudes, temperatures, wind components, and runway gradients, as applicable within the operational limits of the airplane. Each case must include conditions of power, configuration, speed, and the procedures for handling. Also, performance information of climbing performance must be furnished for climb in landing and approach configurations.[10]

AC 25.1581 is the FAA advisory circular that expands the understanding of what the agency desires from the Airplane Flight Manual. While the AC's do present clearer instruction for the assembly of an AFM, they are not mandatory and do not constitute a requirement. Even though they are not mandatory, the FAA prefers seeing them met because they are derived from industry experience in determining compliance with airworthiness standards.[24]

AC 25.1581 states that the AFM should be limited to the smallest practicable amount of material that is appropriate for the intended operation of the airplane and said information should be uniquely related to safety or airworthiness. This AC also reiterates the need of segregation between FAA-approved and non-FAA-approved.[24]

AC 25.1581 Takeoff Flight Path Data states, "Takeoff flight paths, or performance information necessary to construct such paths, together with the associated conditions should be presented for each approved takeoff configuration throughout the approved takeoff operating envelope." This AC also advises that the flight path data is presented so that the net flight path can be determined up to 3,000 ft. above the takeoff surface, instead of the required 1,500 ft. The rationale for this expansion of data is for, "obstacle clearance analysis for distant obstacles of considerable elevation that may be encountered in operations from mountain airports." Regarding obstacle clearance

determination, "Climb gradient decrements for bank angles up to at least 15 degrees should be provided in the AFM. Consider providing coverage of higher bank angles as appropriate to the expected operation of the airplane."[22] For the enroute flight path, data must be provided for AEO and OEI configurations throughout the approved operating altitudes and temperatures.

While these regulations and advisements have ensured a high level of safety, they do not specifically require insight to the full performance envelope of an aircraft. One gap in the knowledge of aircraft performance is banking turns in relation to climb performance and obstacle clearance. Regulations and advisements suggest that data should be provided for bank angles up to 15 degrees. Any bank beyond 15 degrees is not specifically required or advised by the requirements covered thus far. However, the manufacturer must present information that would necessary to counteract a failure that would result in catastrophic failure. In the event that an aircraft must clear an obstacle and in order to do so must bank beyond 15 degrees, there may not be the performance data for the turn required to clear the obstacle. Autopilot controls in a Boeing 737 offer bank angle settings of 15º, 20º, 25º, and 30º. This allows for more aggressive maneuvers, but unless the pilot manually controls the aircraft the turn-climb performance is restricted to these autopilot settings.

D. Obstacle Avoidance

AC-120-91 exists to describe the acceptable methods for developing takeoff and initial climb-out airport obstacle and in-flight procedures to comply with the regulations set forth by the FAA. AC-120-91 notes that there is detailed discussion within the CFR in determining vertical clearance, but little guidance pertaining to lateral separation. AC-120-91 also notes that Standard Instrument Departures (SID) based on Terminal Instrument Procedures (TERPS) operate off the assumption that the aircraft is in normal, fully functional condition (AEO) making SIDs based on TERPS irrelevant in the case of OEI. Special routing for OEI scenarios are made to circumvent a possible problem. Compliance with OEI requirements may not satisfy TERPS requirements and compliance with AEO TERPS requirements may not satisfy OEI obstacle avoidance requirements.[23] An optimal departure should be found that can fulfil the requirements of both.

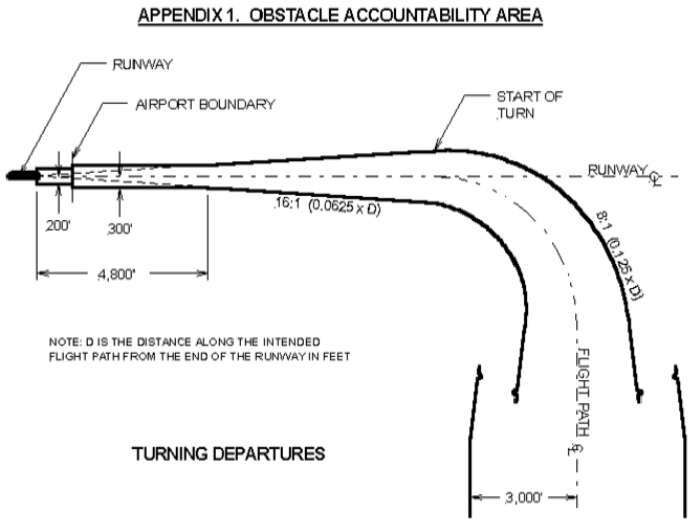

Figure 7. OAA Calculation Example from AC-120-91. *This figure shows the general calculation of an OAA for an intended flight track that includes a turn.*

Also, obstacle avoidance analysis is based off the net takeoff flightpath which carries the implied pessimism of the CFR. The FAA requires that the net takeoff flight path must clear all obstacles by either 35 ft. vertically, or 200 ft. laterally inside airport boundaries, or 300 ft. laterally outside the airport boundaries. AC-120-91 offers two methods of avoidance the Area Analysis Method and the Flight Track Analysis Method. Using the Area Analysis Method, an Obstacle Accountability Area (OAA) is described as a section centered on the runway in which all obstacles must be cleared vertically. Two methods for calculating the dimensions of the OAA are presented for intended flight paths that are straight and for those which include a turn. The general OAA schematic for an intended flight track with a turn is shown in Figure 7. OAA analysis implies that bank angle and speed are varied to keep the turn radius constant. In practice an avoidance maneuver may not be performed with a constant turn radius. AC-120-91 also states that, "no accountability is needed for the radius of turn or gradient loss in the turn for a turn with a 15 degree of less change in heading." These simplifications offer a reasonable level of safety due to the size of the OAA.[25]

AC-120-91 gives guidance of the factors that influence turns. It reminds the reader that winds must be accounted for in a turn. For small heading changes this is not a huge issue, but in the case of larger turns (i.e. 90 degrees) the change in the direction of oncoming wind is substantial. Temperature also has a noticeable effect on turn radius and airspeed thus affecting TAS and WAT limits.[25]

The AC also admits that banking beyond 15 degrees may enhance obstacle clearance for certain airports. Consequently, obstacle avoidance can be an issue at these airports. Maximum allowable bank angles are defined throughout climb by AC-120-91. Under an altitude of 50 ft., no bank angle may be used. Between 50ft. – 100ft. above ground the aircraft may bank up to 15 degrees. Between 100ft. – 400ft. the aircraft may bank 20 degrees, and thereafter may bank up to 25 degrees. If an operator wishes to bank an aircraft past 25 degrees, it requires a specific evaluation and approval from the FAA. These maximum bank angles are tabulated and displayed in Figure 8.

MAXIMUM BANK ANGLES

Height (above Departure End of Runway - feet)	Maximum Bank Angle (degrees)
h>400	25
400>h>100	20
100>h>50*	15

Figure 8. Maximum Bank Angles Allowed from AC-120-91. *This table shows the maximum bank angle as a function of altitude as prescribed by AC-120-91. The asterisk designates that if half the wingspan is greater 50 ft., it becomes the minimum height above ground at which the aircraft can begin to bank.*

BANK ANGLE ADJUSTMENTS

Bank Angle	Speed	'G' Load	Gradient Loss
15°	V_2	1.035	AFM 15° Gradient Loss
20°	V_2+XX/2	1.064	Double 15° Gradient Loss
25°	V_2+XX	1.103	Triple 15° Gradient Loss

Figure 9. Gradient Degradation and Decision Speed Adjustments from AC-120-91. *This figure shows the advised adjustments to V_2 and climb gradient degradation for bank angles above 15 degrees. XX represents the AEO operating speed increment. (Approximately 10 or 15 knots)*

AC-120-91 provides some guidance on the climb degradation due to banking. It states that AFMs generally provide decrements to climb gradient up to 15 degrees of bank and that that decrement may be scaled proportionally to model bank angles below 15 degrees. If the aircraft must bank beyond 15 degrees additional degradation must be applied. When banking beyond 15 degrees, V_2 speeds should be increased to provide an equivalent level of stall margin and adequate controllability. The AC also provides a variation for V_2 speeds for different bank angles. These adjustments are shown in Figure 9. Unless otherwise specified by the AFM or the manufacturer, these adjustments are to be used to anticipate turn-climb performance of an aircraft.[25]

The requirements and ACs outline a sufficient level of understanding that ensures a high level of safety. Aircraft are known for their safety and this is directly correlated to the requirements, regulations, and advisement set forth by the FAA. However, the variations of charts presented and approved in AFMs can be quite large. There is also a low level of consistency between the presentations of data within different manufacturer's AFMs. In the next section charts from various aircraft are presented to illustrate the difference in AFMs and also highlight the need for a deeper understanding of turning while climbing.

III. Excerpts from Aircraft Performance Manuals

The performance data furnished in this study was found throughout Aircraft Flight Manuals (AFMs)[26,27,28], Flight Planning Performance Manuals (FPPMs), and Flight Crew Operating Manuals (FCOMs)[29]. Examination of these manuals has shown no standard in the presentation of performance data amongst manufacturers. Each manual contains different styles and types of data. All the manuals were required to fully document a single aircraft's performance. Unfortunately, there is no universal manual with all the performance data. Tables and charts are the main presentation methods of data, each has its own appeal and drawback. The precision and accuracy of data collection by dispatch or a pilot is affected by the choice of presentation which is made by the designer.

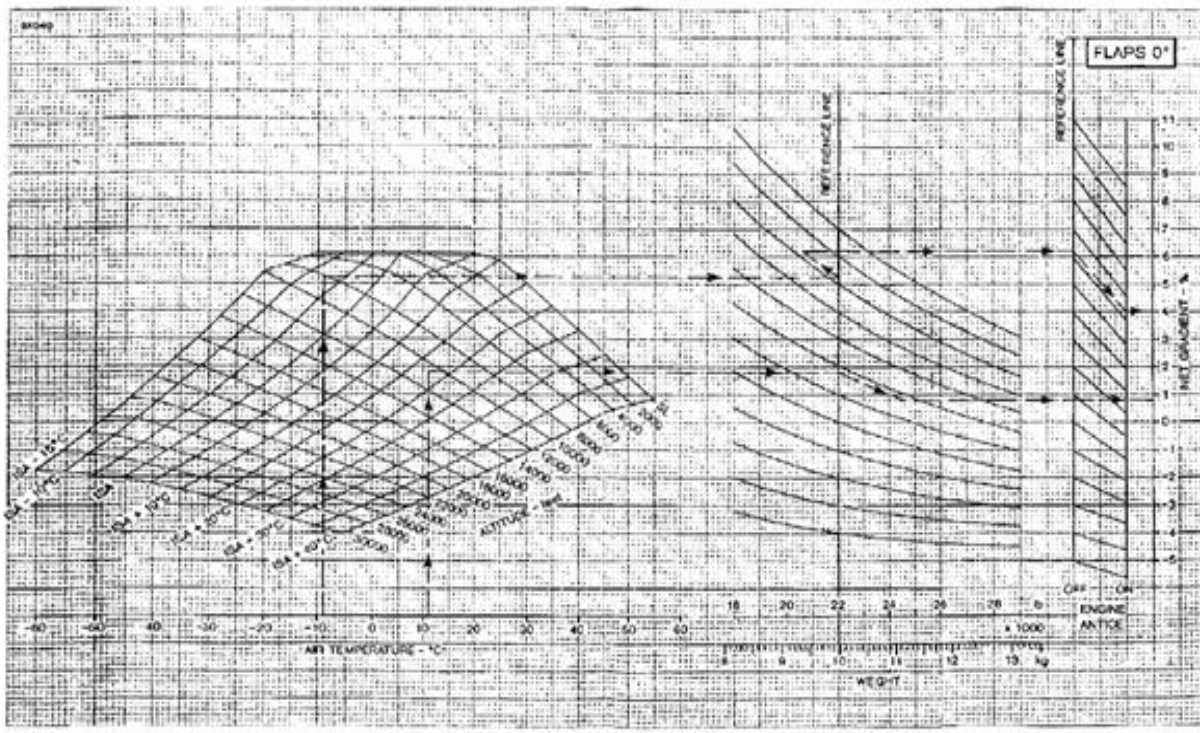

Figure 10. Net Climb Gradient Chart from Hawker 800 XP AFM. *This chart shows the effects of altitude, temperature, weight, flap setting, and engine anti-ice setting on net gradient in OEI conditions. There is no mention of bank angle in this chart of net gradient performance.*

In performance charts, it is common practice to chase through multiple curves to arrive at the final value of interest. Each curve leading to the final value represents a variation of a different flight condition. Figure 10 is the enroute OEI net climb gradient performance chart for the Hawker 800XP with no flap deflection.[26] The reader enters the chart using the ambient air temperature and altitude, then proceeds through a curve for the variation due to weight. After these curves, a final curve for anti-ice setting is followed, or ignored, to yield the enroute OEI climb gradient with no flap deflection.

Other manufacturers provide tabular data to document the climb performance of their aircraft. A table of second segment climb performance for the Cessna Citation Sovereign Model 680 is provided in Figure 11 (overleaf).[27] Figure 11 is a single page from about 80 pages of climb performance data. The charts include climb performance for first, second, and enroute segments of takeoff. A set of tables is provided for constant: flap deflection, anti-ice setting, airspeed, speedbrake position, landing gear position, and OEI configuration. Data sets are provided for 7˚ and 15˚ flap settings, and anti-ice settings for each segment of climb. Within each data set, climb gradients are documented as functions of altitude, temperature, component of oncoming winds, and weight.

The Cessna tables provide precise values for climb gradient for a large range of altitudes, weights, wind components, temperature, and settings. In total there is a generous amount of climb gradient data. With the large number of data points, interpolation between points would allow dispatchers to investigate intermediate conditions. However, without an actual chart the operators don't gain a feel for the aircraft's dynamic performance. It is easier to get an understanding from the charts than from tabulated data. Conversely, charts do not yield precise values, but give the reader a better feel for the performance since the data is visualized. In tabulated data, reader is simply told the value of interest instead of seeing the totality of the performance. In both cases finding the value of interest is tedious and in the case of emergency would take much too long to find any useful information. It falls on the ground operators to properly schedule a mission and provide adequate emergency procedures to minimize risk.

SECOND SEGMENT TAKEOFF NET CLIMB GRADIENT - PERCENT
FLAPS - 15°

CONDITIONS: ANTI-ICE - ON
LANDING GEAR - UP
AIRSPEED - V2

SPEEDBRAKES - RETRACT
INOPERATIVE ENGINE - WINDMILLING
OPERATIVE ENGINE - TAKEOFF THRUST

ALT FT	TEMP DEG C	WEIGHT - POUNDS																								
		30000					29000					28000					27000					26000				
		WIND KNOTS					WIND KNOTS					WIND KNOTS					WIND KNOTS					WIND KNOTS				
		-10	0	10	20	30	-10	0	10	20	30	-10	0	10	20	30	-10	0	10	20	30	-10	0	10	20	30
0	-54	4.2	5.0	5.3	5.8	6.0	4.9	5.7	6.1	6.5	6.9	5.4	6.4	6.8	7.2	7.7	6.0	7.1	7.5	8.0	8.5	6.7	7.8	8.3	8.8	9.4
	-50	4.2	5.0	5.3	5.6	6.0	4.9	5.7	6.1	6.5	6.9	5.5	6.4	6.8	7.2	7.7	6.1	7.1	7.5	8.0	8.5	6.7	7.9	8.3	8.8	9.4
	-45	4.2	5.0	5.3	5.6	5.9	4.9	5.8	6.1	6.5	6.9	5.5	6.4	6.8	7.2	7.7	6.1	7.1	7.5	8.0	8.5	6.7	7.9	8.3	8.8	9.4
	-40	4.3	5.0	5.3	5.6	5.9	4.9	5.8	6.1	6.5	6.9	5.5	6.4	6.8	7.2	7.7	6.1	7.1	7.5	8.0	8.5	6.7	7.9	8.3	8.8	9.4
	-35	4.3	5.0	5.3	5.6	5.9	4.9	5.8	6.1	6.5	6.9	5.5	6.4	6.8	7.2	7.7	6.1	7.1	7.5	8.0	8.5	6.7	7.9	8.3	8.8	9.4
	-30	4.3	5.0	5.3	5.6	5.9	5.0	5.8	6.1	6.5	6.9	5.5	6.4	6.8	7.2	7.6	6.1	7.1	7.5	8.0	8.5	6.8	7.9	8.3	8.8	9.4
	-25	4.3	5.0	5.3	5.8	5.9	5.0	5.8	6.1	6.5	6.9	5.5	6.4	6.8	7.2	7.6	6.1	7.1	7.5	8.0	8.5	6.8	7.9	8.3	8.8	9.4
	-20	4.3	5.0	5.3	5.6	5.9	5.0	5.8	6.1	6.5	6.9	5.6	6.5	6.8	7.2	7.6	6.2	7.2	7.5	8.0	8.5	6.8	7.9	8.3	8.8	9.4
	-15	4.3	5.0	5.3	5.6	5.9	5.0	5.8	6.1	6.5	6.9	5.6	6.5	6.8	7.2	7.6	6.2	7.2	7.6	8.0	8.5	6.8	7.9	8.4	8.8	9.4
	-10	4.3	5.0	5.3	5.6	5.9	5.0	5.8	6.1	6.5	6.9	5.6	6.5	6.8	7.2	7.6	6.2	7.2	7.6	8.0	8.5	6.8	7.9	8.4	8.8	9.4
	-5	4.3	5.0	5.3	5.6	5.9	5.0	5.8	6.1	6.5	6.9	5.6	6.5	6.8	7.2	7.6	6.2	7.2	7.6	8.0	8.5	6.9	7.9	8.4	8.8	9.4
	0	4.3	5.0	5.2	5.5	5.9	5.0	5.8	6.1	6.4	6.8	5.5	6.4	6.7	7.1	7.5	6.1	7.1	7.5	7.9	8.4	6.8	7.9	8.3	8.7	9.3
	5	3.6	4.2	4.4	4.7	5.0	4.3	5.0	5.2	5.5	5.8	4.6	5.6	5.9	6.2	6.6	5.4	6.2	6.6	6.9	7.3	6.0	7.0	7.3	7.7	8.2
	10	2.9	3.4	3.6	3.8	4.1	3.6	4.1	4.4	4.6	4.9	4.1	4.7	5.0	5.3	5.6	4.6	5.4	5.7	6.0	6.3	5.2	6.0	6.4	6.7	7.1
1	-54	4.2	4.9	5.2	5.5	5.9	4.8	5.7	6.0	6.4	6.8	5.4	6.3	6.7	7.1	7.6	6.0	7.0	7.4	7.9	8.4	6.8	7.8	8.2	8.7	9.3
0	-50	4.2	4.9	5.2	5.5	5.9	4.9	5.7	6.0	6.4	6.8	5.4	6.3	6.7	7.1	7.6	6.0	7.0	7.4	7.9	8.4	6.8	7.8	8.2	8.7	9.3
0	-45	4.2	4.9	5.2	5.5	5.8	4.9	5.7	6.0	6.4	6.8	5.4	6.3	6.7	7.1	7.6	6.0	7.0	7.4	7.9	8.4	6.7	7.8	8.2	8.7	9.3
0	-40	4.2	4.9	5.2	5.5	5.8	4.9	5.7	6.0	6.4	6.8	5.4	6.3	6.7	7.1	7.5	6.0	7.0	7.4	7.9	8.4	6.7	7.8	8.2	8.7	9.3
	-35	4.2	4.9	5.2	5.5	5.8	4.9	5.7	6.0	6.4	6.8	5.5	6.3	6.7	7.1	7.5	6.1	7.0	7.4	7.9	8.4	6.7	7.8	8.2	8.7	9.3
	-30	4.2	4.9	5.2	5.5	5.8	4.9	5.7	6.0	6.4	6.8	5.5	6.4	6.7	7.1	7.5	6.1	7.1	7.4	7.9	8.4	6.7	7.8	8.2	8.7	9.3
	-25	4.2	4.9	5.2	5.5	5.8	4.9	5.7	6.0	6.4	6.8	5.5	6.4	6.7	7.1	7.5	6.1	7.1	7.5	7.9	8.4	6.7	7.8	8.2	8.7	9.3
	-20	4.3	4.9	5.2	5.5	5.8	4.9	5.7	6.0	6.4	6.8	5.5	6.4	6.7	7.1	7.5	6.1	7.1	7.5	7.9	8.4	6.7	7.8	8.3	8.7	9.2
	-15	4.3	5.0	5.2	5.5	5.8	5.0	5.7	6.0	6.4	6.8	5.5	6.4	6.7	7.1	7.5	6.1	7.1	7.5	7.9	8.4	6.8	7.8	8.3	8.7	9.2
	-10	4.3	5.0	5.2	5.5	5.8	5.0	5.7	6.0	6.4	6.8	5.5	6.4	6.7	7.1	7.5	6.1	7.1	7.5	7.9	8.4	6.8	7.8	8.3	8.7	9.2
	-5	4.3	5.0	5.2	5.5	5.8	5.0	5.7	6.0	6.4	6.7	5.5	6.4	6.7	7.1	7.5	6.1	7.1	7.5	7.9	8.3	6.8	7.8	8.3	8.7	9.2
	0	4.0	4.7	4.9	5.2	5.5	4.7	5.4	5.7	6.0	6.4	5.2	6.1	6.4	6.7	7.1	5.8	6.7	7.1	7.5	7.9	6.5	7.5	7.9	8.3	8.8
	5	3.4	3.9	4.1	4.3	4.6	4.0	4.6	4.9	5.1	5.4	4.5	5.2	5.5	5.8	6.1	5.1	5.9	6.2	6.5	6.9	5.7	6.6	6.9	7.3	7.7
	10	2.7	3.1	3.3	3.5	3.7	3.3	3.8	4.0	4.3	4.5	3.8	4.4	4.6	4.9	5.2	4.3	5.0	5.3	5.6	5.9	4.9	5.7	6.0	6.3	6.7
2	-54	4.2	4.9	5.2	5.5	5.8	4.8	5.6	6.0	6.3	6.7	5.4	6.3	6.7	7.1	7.5	6.0	7.0	7.4	7.8	8.3	6.6	7.7	8.2	8.7	9.3
0	-50	4.2	4.9	5.2	5.5	5.8	4.8	5.7	6.0	6.3	6.7	5.4	6.3	6.7	7.1	7.5	6.0	7.0	7.4	7.8	8.3	6.6	7.7	8.2	8.7	9.2
0	-45	4.2	4.9	5.2	5.5	5.8	4.9	5.7	6.0	6.3	6.7	5.4	6.3	6.7	7.1	7.5	6.0	7.0	7.4	7.8	8.3	6.7	7.8	8.2	8.7	9.2
0	-40	4.2	4.9	5.2	5.5	5.8	4.9	5.7	6.0	6.3	6.7	5.4	6.3	6.7	7.1	7.5	6.0	7.0	7.4	7.8	8.3	6.7	7.8	8.2	8.7	9.2
	-35	4.2	4.9	5.2	5.5	5.8	4.9	5.7	6.0	6.3	6.7	5.4	6.3	6.7	7.1	7.5	6.0	7.0	7.4	7.8	8.3	6.7	7.8	8.2	8.7	9.2
	-30	4.2	4.9	5.2	5.5	5.8	4.9	5.7	6.0	6.3	6.7	5.5	6.3	6.7	7.1	7.5	6.1	7.0	7.4	7.8	8.3	6.7	7.8	8.2	8.7	9.2
	-25	4.2	4.9	5.2	5.5	5.8	4.9	5.7	6.0	6.3	6.7	5.5	6.3	6.7	7.1	7.5	6.1	7.0	7.4	7.8	8.3	6.7	7.8	8.2	8.7	9.2
	-20	4.3	4.9	5.2	5.5	5.8	4.9	5.7	6.0	6.3	6.7	5.5	6.4	6.7	7.1	7.5	6.1	7.0	7.4	7.8	8.3	6.7	7.8	8.2	8.7	9.2
	-15	4.3	4.9	5.2	5.5	5.8	4.9	5.7	6.0	6.3	6.7	5.5	6.4	6.7	7.1	7.5	6.1	7.1	7.4	7.8	8.3	6.8	7.8	8.2	8.7	9.2
	-10	4.3	4.9	5.2	5.5	5.8	5.0	5.7	6.0	6.3	6.7	5.5	6.4	6.7	7.1	7.5	6.1	7.1	7.4	7.8	8.3	6.8	7.8	8.2	8.7	9.2
	-5	4.3	4.9	5.2	5.5	5.8	5.0	5.7	6.0	6.3	6.7	5.5	6.4	6.7	7.1	7.5	6.1	7.1	7.4	7.8	8.3	6.8	7.8	8.2	8.7	9.2
	0	3.7	4.3	4.5	4.8	5.1	4.4	5.1	5.3	5.8	5.9	4.9	5.7	6.0	6.3	6.7	5.5	6.4	6.7	7.0	7.4	6.1	7.1	7.4	7.8	8.3
	5	3.1	3.6	3.7	4.0	4.2	3.7	4.3	4.5	4.7	5.0	4.2	4.9	5.1	5.4	5.7	4.8	5.5	5.8	6.1	6.5	5.4	6.2	6.5	6.9	7.3
	10	2.4	2.8	3.0	3.2	3.4	3.0	3.5	3.7	3.9	4.1	3.5	4.1	4.3	4.5	4.8	4.1	4.7	4.9	5.2	5.5	4.8	5.3	5.6	5.9	6.3
3	-54	4.2	4.9	5.2	5.5	5.8	4.9	5.7	6.0	6.3	6.7	5.4	6.3	6.7	7.1	7.5	6.0	7.0	7.4	7.8	8.3	6.7	7.8	8.2	8.7	9.2
0	-50	4.2	4.9	5.2	5.5	5.8	4.9	5.7	6.0	6.3	6.7	5.4	6.3	6.7	7.1	7.5	6.0	7.0	7.4	7.8	8.3	6.7	7.8	8.2	8.7	9.2
0	-45	4.2	4.9	5.2	5.5	5.8	4.9	5.7	6.0	6.3	6.7	5.4	6.3	6.7	7.1	7.5	6.0	7.0	7.4	7.8	8.3	6.7	7.8	8.2	8.7	9.2
0	-40	4.2	4.9	5.2	5.5	5.8	4.9	5.7	6.0	6.3	6.7	5.5	6.3	6.7	7.1	7.5	6.1	7.0	7.4	7.8	8.3	6.7	7.8	8.2	8.7	9.2
	-35	4.2	4.9	5.2	5.5	5.8	4.9	5.7	6.0	6.3	6.7	5.5	6.3	6.7	7.1	7.5	6.1	7.0	7.4	7.8	8.3	6.7	7.8	8.2	8.7	9.2
	-30	4.2	4.9	5.2	5.5	5.8	4.9	5.7	6.0	6.3	6.7	5.5	6.4	6.7	7.1	7.5	6.1	7.1	7.4	7.8	8.3	6.7	7.8	8.2	8.7	9.2
	-25	4.3	4.9	5.2	5.5	5.8	4.9	5.7	6.0	6.3	6.7	5.5	6.4	6.7	7.1	7.5	6.1	7.1	7.4	7.9	8.3	6.8	7.8	8.2	8.7	9.2
	-20	4.3	4.9	5.2	5.5	5.8	5.0	5.7	6.0	6.3	6.7	5.5	6.4	6.7	7.1	7.5	6.1	7.1	7.4	7.8	8.3	6.8	7.8	8.2	8.7	9.2
	-15	4.3	4.9	5.2	5.5	5.8	5.0	5.7	6.0	6.4	6.7	5.5	6.4	6.7	7.1	7.5	6.1	7.1	7.4	7.9	8.3	6.8	7.8	8.2	8.7	9.2
	-10	4.3	5.0	5.2	5.5	5.8	5.0	5.7	6.0	6.4	6.7	5.6	6.4	6.7	7.1	7.5	6.2	7.1	7.5	7.9	8.3	6.8	7.8	8.2	8.7	9.2
	-5	4.1	4.7	5.0	5.2	5.5	4.8	5.5	5.8	6.1	6.4	5.3	6.1	6.5	6.8	7.2	5.9	6.8	7.2	7.6	8.0	6.6	7.6	8.0	8.4	8.9
	0	3.4	4.0	4.2	4.4	4.7	4.1	4.7	4.9	5.2	5.5	4.6	5.3	5.6	5.9	6.2	5.2	6.0	6.3	6.6	7.0	5.8	6.7	7.0	7.4	7.8
	5	2.8	3.2	3.4	3.6	3.8	3.4	3.9	4.1	4.4	4.6	3.9	4.5	4.7	5.0	5.3	4.5	5.1	5.4	5.7	6.0	5.0	5.8	6.1	6.4	6.8
	10	2.2	2.5	2.7	2.8	3.0	2.8	3.2	3.4	3.6	3.8	3.3	3.8	4.0	4.2	4.4	3.8	4.4	4.6	4.8	5.1	4.3	5.0	5.3	5.6	5.9
4	-54	4.2	4.9	5.2	5.5	5.8	4.9	5.7	6.0	6.4	6.8	5.5	6.4	6.7	7.1	7.5	6.1	7.1	7.4	7.9	8.4	6.7	7.8	8.2	8.7	9.3
0	-50	4.2	4.9	5.2	5.5	5.8	4.9	5.7	6.0	6.4	6.8	5.5	6.4	6.7	7.1	7.5	6.1	7.1	7.5	7.9	8.4	6.7	7.8	8.2	8.7	9.3
0	-45	4.3	4.9	5.2	5.5	5.8	4.9	5.7	6.0	6.4	6.8	5.5	6.4	6.7	7.1	7.5	6.1	7.1	7.5	7.9	8.4	6.8	7.8	8.3	8.7	9.2
0	-40	4.3	4.9	5.2	5.5	5.8	5.0	5.7	6.0	6.4	6.8	5.5	6.4	6.7	7.1	7.5	6.1	7.1	7.5	7.9	8.3	6.8	7.8	8.3	8.7	9.2
	-35	4.3	5.0	5.2	5.5	5.8	5.0	5.7	6.0	6.4	6.7	5.5	6.4	6.7	7.1	7.5	6.1	7.1	7.5	7.9	8.3	6.8	7.8	8.3	8.7	9.2
	-30	4.3	5.0	5.2	5.5	5.8	5.0	5.8	6.1	6.4	6.8	5.6	6.4	6.7	7.1	7.5	6.2	7.1	7.5	7.9	8.3	6.8	7.9	8.3	8.7	9.2
	-25	4.3	5.0	5.2	5.5	5.8	5.0	5.8	6.1	6.4	6.7	5.6	6.4	6.7	7.1	7.5	6.2	7.1	7.5	7.9	8.3	6.8	7.9	8.3	8.7	9.2
	-20	4.3	5.0	5.2	5.5	5.8	5.0	5.8	6.1	6.4	6.8	5.6	6.4	6.8	7.1	7.5	6.2	7.1	7.5	7.9	8.3	6.9	7.9	8.3	8.7	9.2
	-15	4.3	5.0	5.3	5.5	5.8	5.0	5.8	6.1	6.4	6.8	5.6	6.4	6.8	7.1	7.5	6.2	7.1	7.5	7.9	8.3	6.9	7.9	8.3	8.7	9.2
	-10	4.4	5.0	5.3	5.5	5.8	5.0	5.8	6.1	6.4	6.7	5.6	6.4	6.8	7.1	7.5	6.2	7.1	7.5	7.9	8.3	6.9	7.9	8.3	8.7	9.2
	-5	3.8	4.4	4.6	4.8	5.1	4.5	5.1	5.4	5.7	6.0	5.0	5.7	6.0	6.3	6.7	5.6	6.4	6.7	7.1	7.5	6.2	7.1	7.5	7.9	8.3
	0	3.1	3.6	3.8	4.0	4.2	3.8	4.3	4.6	4.8	5.1	4.3	4.9	5.2	5.5	5.8	4.9	5.6	5.9	6.2	6.5	5.5	6.3	6.6	6.9	7.3
	5	2.5	2.9	3.1	3.2	3.4	3.1	3.6	3.8	4.0	4.2	3.6	4.1	4.4	4.6	4.9	4.1	4.8	5.0	5.3	5.6	4.7	5.4	5.7	6.0	6.3
	10	1.9	2.2	2.4	2.5	2.7	2.5	2.9	3.1	3.2	3.4	3.0	3.4	3.6	3.8	4.1	3.5	4.0	4.2	4.5	4.7	4.0	4.7	4.9	5.2	5.5

Figure 4-453-1 (Sheet 1 of 8)

Figure 11. Cessna Citation Sovereign Model 680 Climb Performance Chart. *This table documents the climb net climb gradient for the Cessna Citation Model 680 in the second segment of climb. The parameters unique to this set of tables are: 15 degrees flap deflection, anti-ice is on, the landing gear is retracted, one engine is inoperative while the other produces takeoff thrust, and speedbrakes are retracted.*

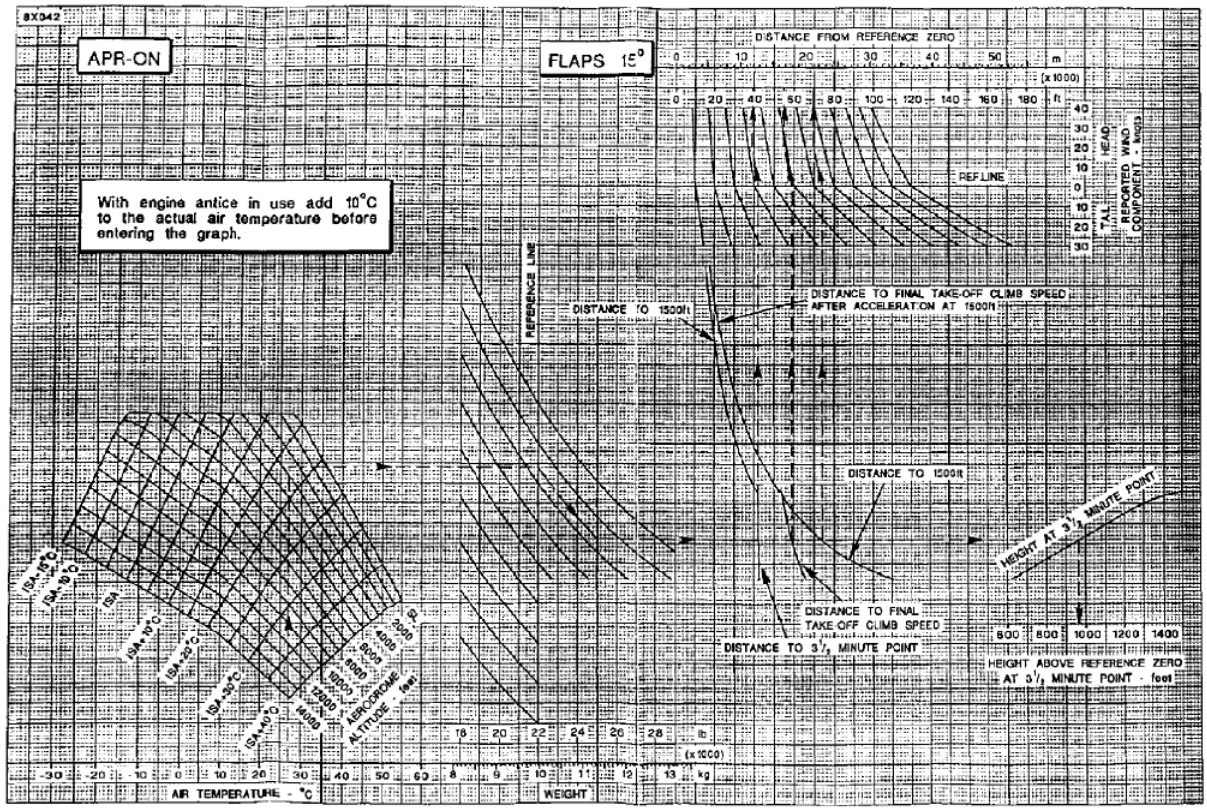

Figure PER-54. Net Takeoff Flight Path—Second, Third and Fourth Segments (Flaps 15°)

Figure 12. Hawker 800XP Net Takeoff Flight Path Data Chart. *This chart shows the required climb gradient needed to avoid a certain obstacle far from the point where final segment begins 400 ft. above the runway surface.*

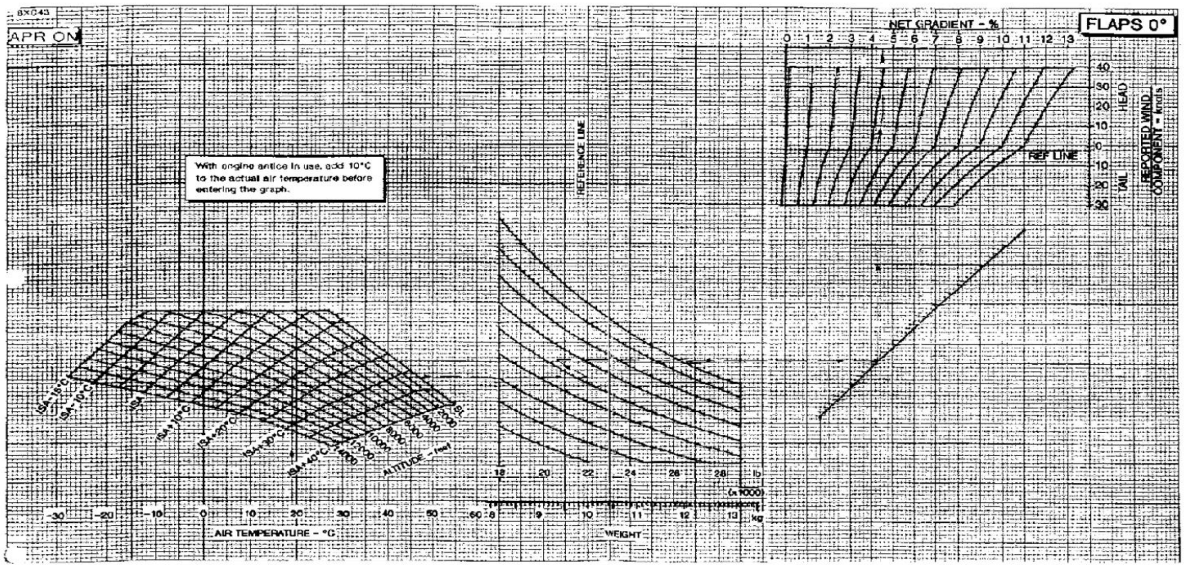

Figure PER-55. Net Takeoff Flight Path—Second Segment Net Gradient (Flaps 0°)

Figure 13. Hawker 800XP Net Takeoff Flight Path Data Chart. *This chart documents the net climb performance of the Hawker 800EX with no flap deflection in the second segment of takeoff. This chart shows variation in net climb gradient as a function of temperature, altitude, and weight.*

Uncertainty affects either method, but in different ways. To what certainty does dispatch know the weight of the aircraft at takeoff and at any point during takeoff? Weight estimations, altitude, temperature, and airspeed all add some uncertainty to the estimated performance of the aircraft. Another factor of uncertainty is the difficulty in obtaining useful data from a performance chart. Figure 12 (above) gives climb performance for all segments of climb, but is rather cryptic in its presentation. Alternatively, separate charts for first, second, and enroute climb performance are also furnished in the Hawker 800XP AFM.[26] The second segment climb performance chart for the Hawker 800XP, shown in Figure 13, is easier to decipher. In Figure 13 (above) the second segment net gradient is documented as a function of temperature, altitude, weight, and wind component. There is no mention of bank angle in this chart of net gradient performance.[26]

These performance charts are integral to safe mission planning. There are also differences in the way obstacle avoidance charts approach the same problem. Figure 14 is a straight out obstacle avoidance chart for the Beechcraft 400.[28] It contains a simple relationship between an obstacle's downrange distance and its height. Figure 14 ultimately gives the required net takeoff gradient for successful obstacle avoidance. Figure 14 covers obstacles up to 1,500 ft. tall and 24 nmi. downrange, which satisfies the CFR requirements but not AC-120-91. While Figure 14 provides required climb gradients, it does not provide the aircraft's actual capabilities. Figure 14 only addresses part of the problem. Boeing gives a more insightful presentation of obstacle avoidance data. A sample of an obstacle limitation chart for the Boeing 737-500 is given in Figure 15 (overleaf).[29] Boeing gives the reader a maximum weight that ensures a certain obstacle will be cleared. The maximum weight is based on the obstacle's height, distance from brake release, ambient temperature, and altitude. Multiple weight decrements are included for various settings as well. Obstacles covered in Figure 15 are up to 1,000 ft. in height which is relatively short knowing that AC-120-91 advises furnishing obstacle clearance data up to 3,000 ft. In Figure 15 there is no mention of airspeed. A modest approximation for the V_2 speed is most likely factored into the final weight results, but the chart makes no mention of the desired climb speed. Doghouse plots do estimate the optimal climbing airspeed and document variation in turn-climb performance due to changes in airspeed.

Performance charts give little guidance on turn-climbs and the effects of banking an aircraft. Figure 16 is from a Hawker 800XP AFM that documents the turn radius achieved by a 15˚ bank as a function of climb speed, temperature, and mean altitude throughout climb.[26] This chart is helpful in figuring the path of the aircraft, but makes no reference to the climb gradient or rate of turn for the maneuver. A later change to the Hawker 800XP AFM states that at a 15˚ bank angle, the climb gradient should be reduced by 1%. This general value makes the future calculations of climb degradation at steeper bank angles simpler in light of AC-120-91. However, if the

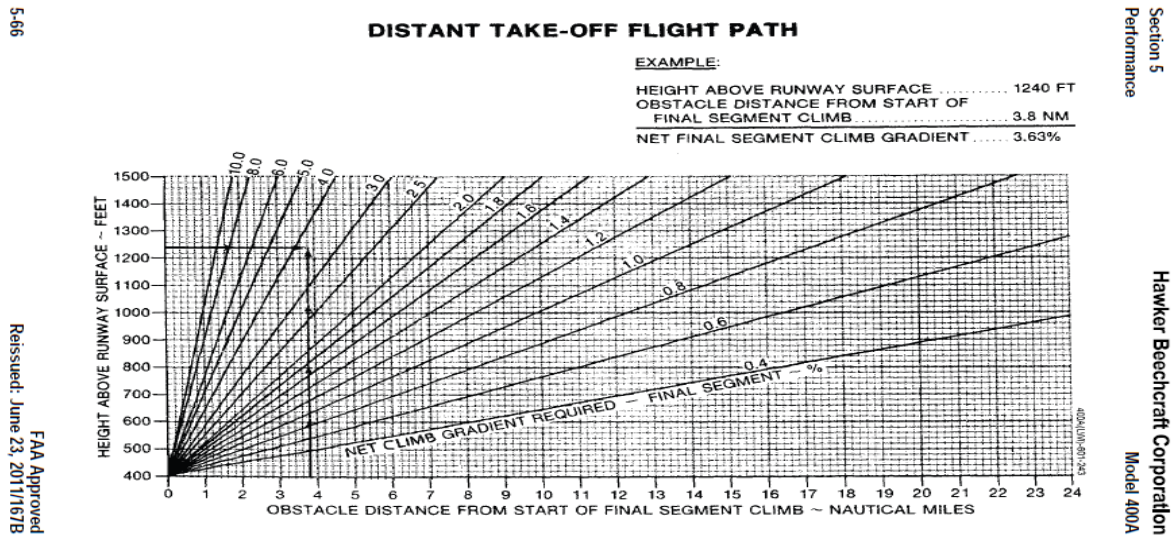

Figure 14. Distant Obstacle Clearance Chart for Beechcraft 400. *This chart shows the required climb gradient needed to avoid a certain obstacle far from the point where final segment begins 400 ft. above the runway surface.*

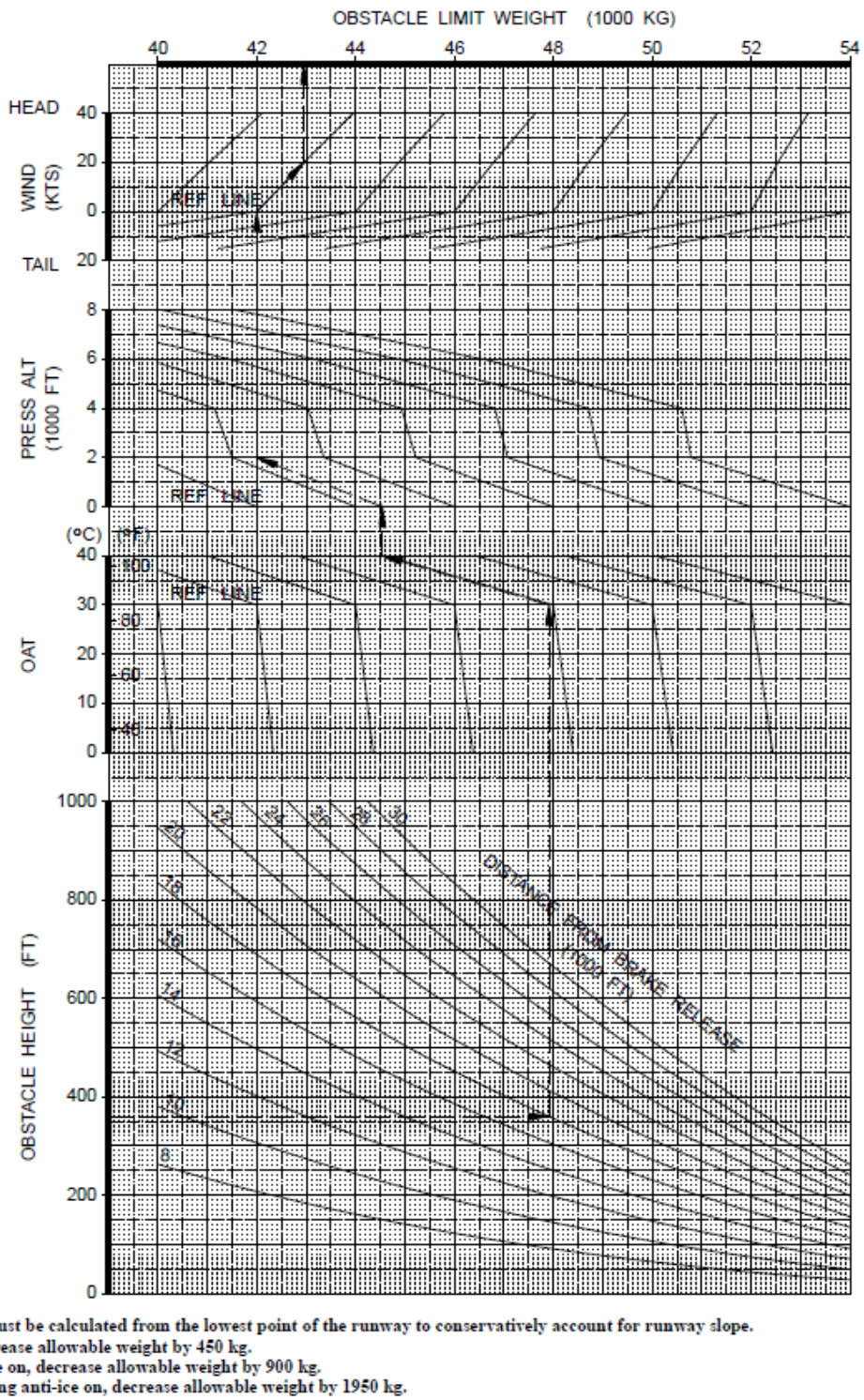

Figure 15. Boeing 737-500 Obstacle Limit Performance Chart. *This chart gives the reader a limit on takeoff weight knowing the position and height of a downrange obstacle. Additional decrements to the weight limit are given for anti-ice and packs settings.*

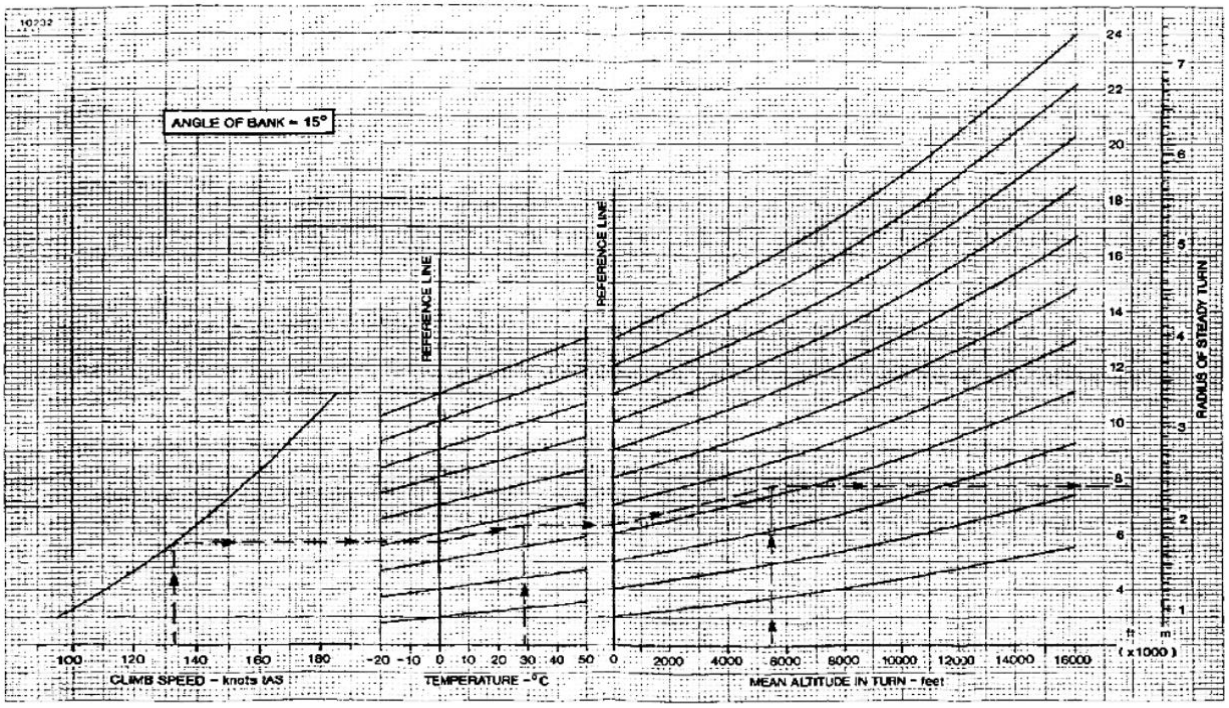

Figure PER-59. Radius of Steady Turn

Figure 16. Hawker 800EX Radius of Steady Turn Performance Chart. *This chart documents the sustained turning performance of the Hawker 800EX. The radius of turn can be found for a given climb speed, temperature, and mean altitude of the maneuver executed at 15 degrees of bank.*

aircraft must bank further than 15˚ Figure 16 loses its value. In the scope of obstacle avoidance, Figure 16 is not precise and offers a range of data too large to be conducive to dispatch.

Boeing provides maneuvering limitations in the long range cruise at a certain Mach number. A sample is provided in Figure 17 (overleaf).[29] Boeing tabulates the maximum altitude that can be sustained for a given bank angle and weight. Figure 17 provides useful information, but is again out of range for use in obstacle avoidance during takeoff. This data seems more applicable for a scenario where the aircraft must change course in cruise to avoid harsh weather or address an emergency situation.

The most applicable figure to the turn-climb problem was found outside of any manual, without any official numbers or approval. In a customer service book, airbus estimates the degradation of climb due to bank angle for a variety of the aircraft.[30] Figure 18 shows the expected loss of climb gradient as a direct function of bank angle. Charts similar to Figure 18 would provide the most insight in the scope of obstacle avoidance during takeoff especially with numbers approved by the manufacturer and the FAA. The advised decrements in AC-120-91 would be passed over for actual data. Dispatch would then be more apt to formulating a truly optimal departure.

This study aims to expand the understanding of obstacle avoidance, specifically in the subject of turn-climbs. For many aircraft, there is no documented performance of turn-climbs and its effects on net takeoff path. In the case aircraft with AFMs that do not provide a deep insight and are assembled with a pessimistic enough view to ensure that safety is very probable, operation of the aircraft may be restricted due to a lack of documented performance. This restriction may be due to ambient temperature, takeoff weight, airport altitude, or the local obstacles. Without plots that document the effects of all of these parameters, it is unclear which will be a limiting factor. It would be the manufacturer's responsibility to assemble more data and go through the process of integrating it into the AFM or getting it approved by the FAA. Reverse engineering credible models for this data can alleviate this issue.

5 Maneuver Capability

LRC AND .74 MACH

WEIGHT	MAXIMUM PRESSURE ALTITUDE (FT) MANEUVER CAPABILITY 'G' (BANK ANGLE)					
1000 LB	1.2 (33°)	1.3 (39°)	1.4 (44°)	1.5 (48°)	1.6 (51°)	1.7 (54°)
140	34200	32600	31000	29500	28000	26700
135	35100	33400	31800	30300	28900	27500
130	35900	34100	32600	31200	29700	28400
125	36700	35000	33500	32000	30500	29200
120		35900	34300	32800	31400	30100
115		36800	35200	33700	32400	31000
110			36100	34700	33400	32000
105				35700	34300	33000
100				36700	35300	34000
95					36400	35200
90						36300

Figure 17. Boeing 737-500 Enroute Maneuvering Capability Chart. *This chart is an excerpt from a Boeing 737 AFM showing the maximum bank angle or G-loading an aircraft can sustain in Long Range Cruise (LRC) at 0.74 Mach at variety of weights and altitudes. Additional charts are furnished for increasing Mach number.*

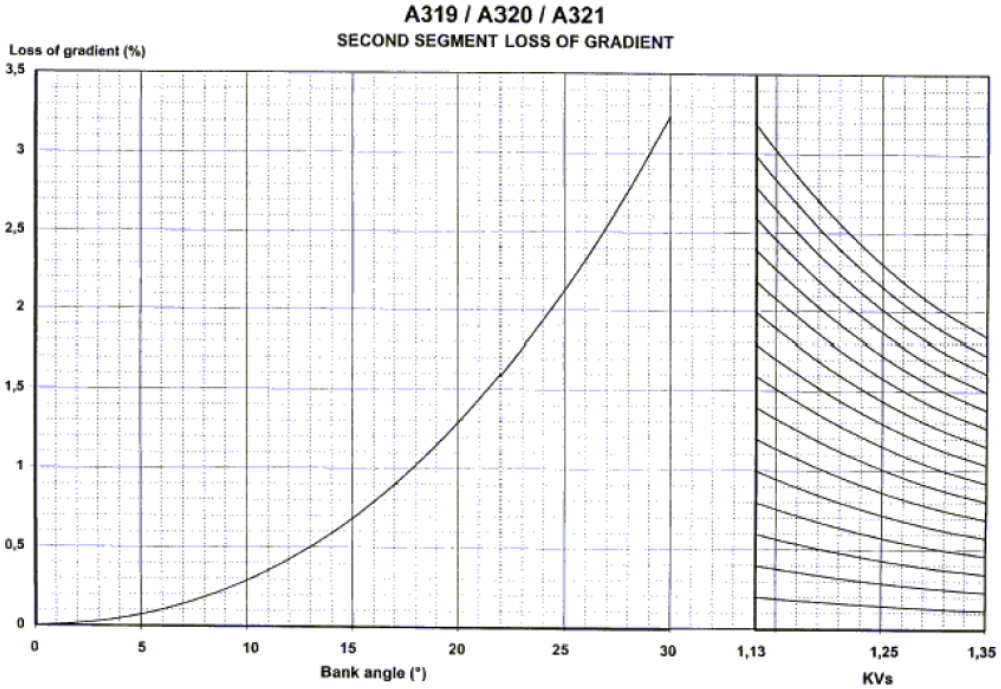

Figure 18. Airbus A320 Family Climb Gradient Lost to Bank Angle Chart. *This chart is a figurative representation of an A320's climb degradation due to bank angle. This chart is not FAA approved and was taken from an Airbus Customer Service book.*

Better methods of presentation can be formulated. Ideally, operators would have access to as much aircraft performance information as possible. The method of presentation, however, is a design choice. By presenting the data in the form of the Doghouse plot we are providing a compact and insightful representation of the data that can be used in real time. Individual plots for weights, altitudes, clean/takeoff configuration, AEO/OEI, can be assembled. At these specific points in the sky, the Doghouse plot clearly shows full turn-climb performance.

IV. Underlying Equations Modelling the Doghouse Plot

The Doghouse plot assesses the coupled effects of turning and climbing. Two distinct models for each type of maneuver are presented in this section. E-M theory is the basis for climbing performance, while simple geometry is used to model the turn an aircraft can achieve. AC 25.1581-1 states that, "Radius of turn, for use in obstacle lateral separation, is not airplane dependent and can easily be calculated from speed and bank angle. Climb gradient decrements, however, are airplane dependent. Climb gradient decrements for bank angles up to at least 15 degrees should be provided in the AFM. Consider providing coverage of higher bank angles as appropriate to the expected operation of the airplane."[24] The Doghouse plot combines these two models into a single plot thereby defining the turn-climb maneuver.

A. Modelling Climb Performance

Inspecting the work-energy theorem, we can model the aircraft using conservation of energy. Taking the time derivative of the energy equation gives an expression in terms of power. It is known that net force multiplied by the velocity of an object is equal to the time rate of change of the energy. Using the small angle approximation, Eq. (1) can be written to describe the conservation of energy. On the right-hand side, there are terms describing the change in potential and kinetic energy. The basic meaning of Eq. (1) is to show that the excess power can be attributed to the change in potential and kinetic energy.[31]

$$(T - D)V = W\frac{dALT}{dt} + \frac{W}{g}\frac{d}{dt}\left(\frac{V^2}{2}\right) \tag{1}$$

It should be noted that the small angle approximation is a reasonable simplification.[33] By assuming a small flight path angle the thrust is modelled to directly counteract drag. For steep flight paths, the effects of thrust offset become significant and more nuance is needed for this model. It should also be noted that weight is assumed constant and is therefore not a function of time. In long range cruise aircraft, this is a valid assumption since any appreciable change in weight is negligible throughout a sustained climb-turn maneuver. For aerodynamic bodies such as missiles the fuel burned throughout a maneuver is very large relative to the total weight. For missiles and other small vehicles, Eq. (1) may not be used as a feasible model of power.

Dividing Eq. (1) by weight yields Eq. (2), which defines the specific excess power.

$$P_s = \frac{(T - D)V}{W} = \frac{dALT}{dt} + \frac{d}{dt}\left(\frac{V^2}{2g}\right) \tag{2}$$

Assuming that the climb is at a constant kinetic energy, we can neglect the last term in Eq. (2)

$$P_s = \frac{(T - D)V}{W} = \frac{dALT}{dt} \approx ROC_{unacclerated} \tag{3}$$

Eq. (3) shows that the unaccelerated ROC is approximately the specific excess power due to its relationship to the change of altitude over time. This is a powerful variant of E-M theory. By assuming that the velocity is or is nearly constant throughout a turn, the specific excess power is directly related to the change in altitude. The amount of excess power an aircraft possesses in a certain configuration completely dictates its ability to climb. However, this version of the ROC is not fully accurate. A linear correction factor is applied in order to compensate for the acceleration induced by climbing at either constant IAS or Mach number as well as the changing conditions of the atmosphere. The form of the true ROC is given in Eq. (4) as,

$$ROC(M, ALT) = K_{accel} \cdot ROC_{unacclerated}(M, ALT) \tag{4}$$

In practice, pilots climb at either constant IAS or constant Mach number. There are instruments for airspeed and Mach number in the cockpit which make it easy for a pilot to do so. There is no instrument, however, to measure the kinetic energy of the aircraft. Therefore, constant kinetic energy climbs are not performed. Since IAS and Mach vary due to changes in the atmosphere, the aircraft's kinetic energy must change in order to hold either IAS or Mach number constant.

The correction constant[31,32,33] is defined in Eq. (5) as:

$$K_{accel} = \frac{1}{1 + \frac{V_{KTAS}(M, ALT)}{g} \cdot \frac{dV_{KTAS}}{dh}(M, ALT)} \tag{5}$$

Applying the 1976 standard atmosphere yield more useable expressions for the accelerated-ROC-correction-factor. While climbing at a constant Mach number, the IAS and TAS will decrease due to the corresponding decrease in ambient temperature. This reduces the local speed of sound. Therefore, the TAS must decrease in order to hold Mach number constant. There are two associated K_{accel} while climbing at constant Mach number. Eq. (6A) gives the correction factor at an altitude below the tropopause and Eq. (6B) gives the correction factor above the tropopause, where the temperature ceases to change with altitude. The tropopause is at an altitude of 36,089 ft.

$$K_{accel} = \frac{1}{1 - 0.133184 \cdot M^2} \tag{6A}$$

$$K_{accel} = 1 \tag{6B}$$

When climbing at a constant IAS, the aircraft will actually need to gain TAS. Since IAS is completely dependent on the density of the air the Pitot tube is reading, IAS will decrease in a constant TAS climb. This is due to the compressibility of air and the change in dynamic pressure with altitude. The correction factor for constant IAS climb are therefore smaller than their constant Mach counterparts. Eq. (7A) gives the correction factor at an altitude below the tropopause and Eq. (7B) gives the correction factor above the tropopause, where the temperature ceases to change with altitude.

$$K_{accel} = \frac{1}{1 + 0.566816 \cdot M^2} \tag{7A}$$

$$K_{accel} == \frac{1}{1 + 0.7 \cdot M^2} \tag{7B}$$

B. Modelling Turn Performance

In a steady turn, no altitude or speed is lost; therefore, vertical forces are balanced. The main component of lift must overcome the gravitational force and thrust must overcome the drag. In order to induce a turn a lateral force must be created. By depressing a wing the lift vector is tilted, creating a component of lift that acts in the lateral plane. This lateral force induces a turn towards the depressed wing.

A steady turn may be modelled as an arc with a constant radius. Remembering basic physics, for an object moving in a circular path there will be an accompanying centripetal acceleration directed towards the center of the circle. Using the two accelerations acting upon the aircraft in a banked turn, the bank angle can be defined. The tangent of the bank angle is describe in Eq. (8) based on the instantaneous airspeed, turn radius, and gravitational acceleration. It should be noted that this model of bank angle is independent of wing geometry, angle of attack, turn rate, and airfoil shape.

$$\tan(\Phi) = \frac{a_c}{g} = \frac{V^2}{g \cdot R} \tag{8}$$

The load factor is defined as the ratio of lifting force over the weight or the gravitational force. Eq. (9) shows useful representations of the load factor in its canonical form.

$$N_z = \frac{L}{W} \quad \rightarrow \quad L = N_z \cdot W \tag{9}$$

Using simple force balancing of a banked aircraft, Eq. (10) can be derived from the balance of the vertical forces. This free-body diagram then implies a direct relationship between the bank angle and load factor.

$$N_z = \frac{1}{\cos(\Phi)} \tag{10}$$

Using trigonometric identities, Eq. (8) can be manipulated into an expression that expresses the turning radius in terms of airspeed and load factor. This expression for turn radius is given in Eq. (11) and can be thought of as the relationship between maneuverability and agility. This representation of the turn radius is crucial to the assembly of the Doghouse plot. Using English units, the gravitational acceleration is defined as 32.174 ft./s^2. The velocity in the numerator refers to the TAS and is converted from knots to ft./s.

$$Turn\ Radius = R = \frac{V^2}{g\sqrt{{N_z}^2 - 1}} = \frac{\left(V_{KTAS} \cdot \frac{6076.12\ {}^{ft}/_{nmi}}{3600\ {}^{s}/_{hr}}\right)^2}{\left(32.174\ {}^{ft}/_{s^2}\right)\sqrt{{N_z}^2 - 1}} \tag{11}$$

Since the turn is modeled as a circle, it is simple to find the turn rate. Taking the ratio of TAS and turn radius gives the turn rate in rad/s. Another simple conversion is applied to change this turn rate into deg/s. The expression for turn rate is given in Eq. (12).

$$Turn\ Rate = \frac{360^o}{2\pi}\left(\frac{V_{KTAS} \cdot \frac{6076.12\ {}^{ft}/_{nmi}}{3600\ {}^{s}/_{hr}}}{R}\right) \tag{12}$$

Since lift equals weight in steady level flight, the maximum instantaneous load factor can be defined as a ratio between the maximum lift coefficient and the instantaneous lift coefficient. The maximum lift coefficient is defined by the maximum angle of attack that the aircraft can achieved before encountering buffeting or stall. Increasing the angle of attack to a point where the flow can no longer stay attached to the top surface of the airfoil defines an upper limit on the lift coefficient achievable by an airfoil. The separated flow will cause the top surface of the wing to lose its low pressure distribution thereby reducing the lift. At higher speeds, buffeting will limit the maximum lift coefficient of the lifting body. Buffeting occurs when the flow is disturbed by a shockwave to the point where substantial eddies are formed. The flow will remain attached to the top surface of the wing, but the flow will induce significant vibrations and oscillatory changes to lift in this regime. Operating with buffeting is detrimental to the aircraft's structure and does not produce any beneficial amount of lift. Considering these two factors, the maximum load factor is defined in Eq. (13).

$$(N_z)_{max}(M, ALT) = \frac{C_{L_{max}}(M)}{C_L(M, ALT)} \tag{13}$$

An expression for the stall speed ratio (SSR) can be expressed in a similar form. Lift coefficient is proportional to the square of the velocity by definition. This proportionality carries through in relation to flight Mach number. An

aircraft is flying near stall at its maximum lift coefficient would have a load factor of 1. The ratio of the stall speed and the incident flight speed can be expressed as the stall speed ratio SSR, given in Eq. (14). The SSR is a useful parameter track since many cue speeds in the CFR are defined in relation to the stall speed.

$$SSR(M, ALT) = \sqrt{\frac{C_{L_{max}}(M)}{C_L(M, ALT)}} \tag{14}$$

C. Models for an Appropriate Reference Frame

The models described in the previous sections are aircraft centric. In obstacle clearance, the ground reference frame is the pertinent reference frame. For proper relation from ground speed to airspeed, wind velocities must be accounted. Any wind changes the TAS, but does not affect the ground speed. The variation in wind velocities affect the operating conditions of the aircraft such as lift and drag. In the aircraft's reference frame, an oncoming headwind would increase the speed of the flow, but will not change the speed of the aircraft relative to ground. In effect a head wind would increase the ROC making the ground reference frame climb gradient steeper. Eq. (15) is the conversion from TAS to ground speed.

$$V_G = V_{KTAS} - V_W \cos\theta \tag{15}$$

While the rates of climb are aircraft centric, the climb gradient is not. Eq. (16) shows the conversion from ROC to climb gradient as,

$$Climb\ Gradient = \frac{ROC(M, ALT)}{V_G} \tag{16}$$

Using the models for turning and climbing performance, the construction of Doghouse plots only require drag polar models and propulsion data of an aircraft. The tools used to obtain these drag polars and the NPSS used to model different engines are discussed in the next section, along with the basic concept of spreadsheet scripting used to generate the data for the Doghouse plot.

V. Constructing Doghouse Plots from First Principles Models

Doghouse plots presented in this study were assembled with reversed engineered performance data. The Doghouse plot presents all required characteristics to completely define a turn-climb maneuver on a single set of axes. Presentation in the form of the Doghouse plot gives a synergistic visualization of turn-climbs and provides more insight than multiple charts or tables. To reverse engineer aircraft performance, drag polar and propulsion estimation programs were used by the authors.

A. Models for Aircraft Drag Polars and Propulsive Systems

Models of the aircraft and propulsion system are needed for accurate representation of performance. Two NASA legacy codes EDET[34] and NPSS[35] were used in the modelling of aircraft's drag polars and turbofan's thrust profiles. This performance model carries minor calibration factors within EDET and NPSS to match documented performance.

Feagin and Morrison developed the Empirical Drag Estimation Technique (EDET) at Lockheed for NASA Ames. EDET is capable of taking simple aircraft dimensions and flight specifications to produce a flat-plate skin-friction drag buildup. EDET also predicts the onset of buffeting and can predict drag polars of an aircraft, all while considering compressibility effects which are expressed as Reynolds number corrections. The lift and drag curves can also be predicted by EDET, but the appeal of EDET is its capability to accurately predict the zero-lift drag of the entire aircraft.[34]

To model an aircraft in EDET, simple aircraft geometry is needed. Wing planform area (S_{ref}), aspect ratio (AR), average wing thickness percentage, quarter-chord sweep, taper ratio, wing wetted area, percentage of camber, wetted area of the fuselage, fuselage length, fuselage fineness ratio, bluff base area, crud-drag factor, reference altitude reference Mach, and addition component geometry (wetted area, length, and thickness-fineness ratio) are all the parameters needed to assemble a flat plate drag model as an input for EDET. These dimensions can be readily found for most aircraft.

NASA's Numerical Propulsion System Simulator (NPSS) can accurately model a two-shaft turbofan engine and tabulate 5-column performance data consisting of net thrust and thrust-specific-fuel-consumption (TSFC) for varying Mach numbers and altitudes.[35]

Openly published specifications were used to calibrate the propulsion simulations. The two-shaft turbofan is simulated using a comprehensive thermodynamic model that considers the compression ratio and efficiency of each stage in the flow path. The NPSS model includes various flow path splitters that govern the bypass ratio. It has specified limits to shaft rpm and turbine inlet temperature. The model balances power developed by the turbine stages and power absorbed by the compressor and/or fan stages. From this thermodynamic model, NPSS develops an estimate of thrust and fuel flow.

The tabular engine performance data comprises thrust and thrust specific consumption, contains the different thrust availabilities, and thrust-specific fuel consumption (TSFC) over a range of altitudes, power levels, and Mach numbers. NPSS varies altitude from sea level to 55,000 feet, Mach of 0 to 1.0, and power level settings of 85% to 100% of $N1_{max}$ (10,000 rpm). Sensitivities to ambient temperature, which are required by the CFR, can be modelled through variations of the propulsion data.

B. Generation of Doghouse Plots

To generate the data needed for the Doghouse plot, turn-climb performance is formulated using load factor and Mach number as independent variables. Bank angle can be inferred from the load factor using Eq. (10). The TAS can then be calculated using the Mach number and the speed of sound. In this formulation, the 1976 Standard Atmosphere is used in finding the speed of sound at the input altitude. Values of turn radius, turn rate, lift coefficient, SSR, drag coefficient, dimensional drag, unaccelerated ROC, constant IAS ROC and constant Mach ROC are calculated and tabulated for each combination of load factor and Mach number. ROC is then converted to climb gradient since climb gradient is common nomenclature for dispatching and compliance with the CFR.

Once data is compiled for load factor and Mach number, turn-climb performance is recast as a function of the dependent variables TAS and turn rate. New axes of arbitrary TAS and turn rate are defined independently. Previous data is then interpolated onto the new grid of TAS and turn rate. Once the data is formatted into functions of TAS and turn rate, a colored contour plot is made for climb gradient while line contour plots are developed for the remaining data. The plots are overlaid thus completing the Doghouse plot. Each Doghouse plot is assembled for a given weight, altitude, flap setting, engine condition, and power level angle (PLA).

Toggling between AEO and OEI conditions requires a simple modification to the original model. In AEO condition, all engines produce thrust and there is no additional drag penalty added to the EDET results. For the OEI configuration, thrust of one engine is neglected and a drag penalty is incorporated for the disabled engine. The drag impact of an inoperative engine is assumed to be a worst-case scenario where the entire fan mechanism is jammed and no airflow is allowed through the engine. In this case, the engine is modelled as a solid wall with area swept out by the fan diameter. The change in zero-lift drag associated with the inoperative engine is given in Eq. (17). Although the engine will most likely be in a windmilling state meaning that air will still be able to flow through the engine, a pessimistic view is used to add an additional buffer between performance and safety.

$$(\Delta C_D)_{inpoperative\ engine} = \frac{(1.0)\left(\pi\frac{d_{fan}{}^2}{4}\right)}{S_{ref}} \tag{17}$$

Variation in flap setting also requires modification to the standard model. Flap deflection effectively adds camber to the airfoil thereby increasing the maximum attainable lift of the section, but decreases the wing's span

efficiency. With its flaps deployed an aircraft can achieve a higher maximum lift coefficient than the maximum limited by buffet boundary and flow separation. The buffet boundary is also changed with flap deflection because the angle of attack needed to achieve higher lift is reduced. The Doghouse model toggles flap configurations. With the flaps deployed, there is an increment of drag associated with the physical obstruction of flow and also an increment associated with the increase in induced drag. By extending the flaps, the lift distribution becomes less elliptical, decreasing the efficiency of the lifting body. To model this the span efficiency, e, is reduced. Equation (18) gives the parabolic model of induced drag is used by EDET and this model.

$$C_{Di} = \frac{{C_L}^2}{\pi\, AR\, e} \tag{18}$$

C. Aerodynamic Model Calibration

The exact aerodynamic performance, such as lift and drag, of an aircraft are usually held proprietary by the manufacturer; there is no published source of aircraft drag polars. It is also unfeasible to interpret the drag polar from performance manuals due to the nature of the published data. However, there is a certain quantity of practicable performance data we can gather from the AFM and other performance manuals to calibrate models.

Since the drag polar cannot be extracted from the AFM, drag polars are estimated by calibrating EDET models to match performance data. Calibration through EDET produces an estimate of an aircraft's drag polar. Empiricism is the best method we have of estimating the performance of an aircraft. A Monte-Carlo optimization was used to vary the span efficiency, crud drag, flap drag, and inoperative engine drag to best match published data for second and fourth segment climb gradients.

There is no general theory estimating the drag and lift due flap deflection. There are many sources that estimate drag due to flap deflection, but are empirical processes. Since methods found have varying results on the accuracy of our model we chose to arbitrarily define the drag increments due to flaps deflection. The same is also true for an inoperative engine, but values were held close to the estimate found using Eq. (17).

Airbus has an electronic performance program, PEP, that delivers the most accurate depiction of their aircrafts' capabilities. Using PEP, the OEI climb gradients for second and fourth segment climb were found and used to calibrate an EDET model. For the Airbus A320, we found that the best fit for the EDET and NPSS model are as follows: e=0.817, CD0_FLAPS=0.0209, CD0_OEI = 0.0135, and CD0_TRIM=0.001.

In the next section, we reverse engineer a Canadair CL600 and an Airbus A320 to illustrate the insight gained by the Doghouse plot.

VI. The Doghouse Plot

Series of Doghouse plots are presented in this section studying the effects of altitude and TOW for two different aircraft. Figures 19, 20, 21 show individual pieces of a Doghouse plot. These plots were assembled using a reverse engineered Airbus a320 and Bombardier CL600.

To read a Doghouse plot, select an airspeed and find the associated bank angle, SSR, and turn radius of interest. At a given speed, bank angle, and SSR the Doghouse plot shows the entire turn-climb performance. The colored contour plot represents the net climb gradient at each point within the operating limits. The reader can

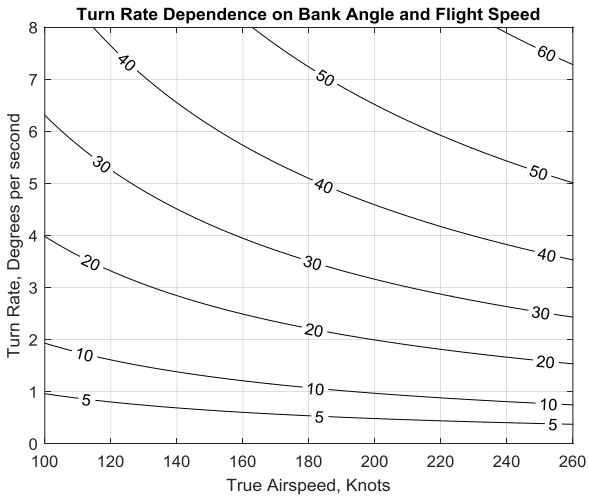

Figure 19. Bank Angle Required to Achieve Specific Turn Rate. *This figure shows the relationship between TAS, bank angle, and the turn rate. Given the general model of a turn, the given bank angles are required to complete a turn at a given speed.*

quickly infer the rate of heading change, the shape of the turn, and the instantaneous climb gradient. The "roof" of the Doghouse plot is formed due to stall limits at low speeds and buffeting at high speeds. In takeoff, the margin between stall and buffeting is large since speed is low.

Currently, there are no plots in any AFM that provide this compact representation of the turn-climb. Using the Doghouse plot, complex problems associated with obstacle avoidance can be simplified. In obstacle avoidance, the required turn rate should be known. Large turn rates can degrade the climb gradient to a point to where the aircraft cannot maintain altitude. From a computational standpoint, a set of simulations can approximate the behavior for a variety of takeoff departures. Using a gradient optimizer along with the Doghouse's raw data, dispatch can optimize departure paths for many scenarios. In the case of obstacle avoidance, it would benefit the operators to simulate avoiding an obstacle both horizontally and vertically to optimize safety margins, or fuel efficiency.

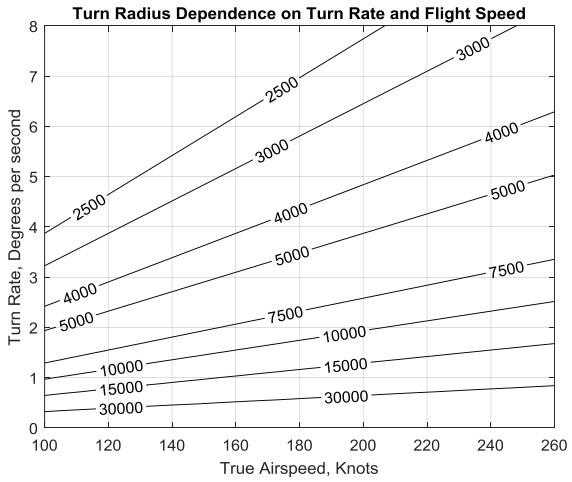

Figure 20. Radius of a Turn Maneuver at a Given Speed and Turn Rate. *This figure shows the relationship between TAS, turn rate, and turn radius. If a certain maneuver is required, the reader can infer the corresponding turn rate*

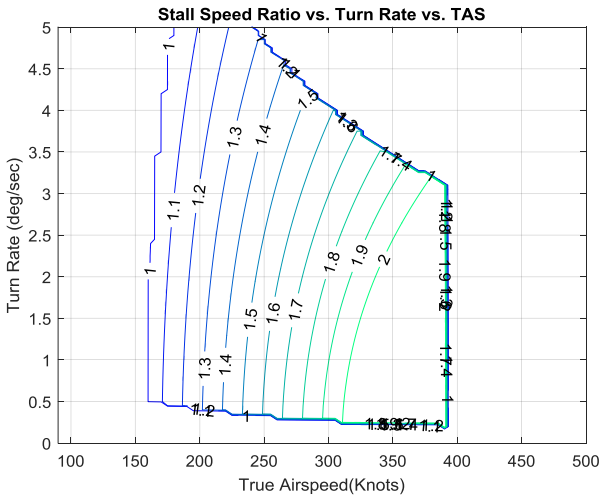

Figure 21. Stall Speed Ratio at a Given Speed and Turn Rate. *This figure shows the relationship between TAS, turn rate, and stall speed ratio. If a certain maneuver is performed, the reader can quickly infer the stall margin from this plot.*

To illustrate this problem refer to Figs. 22-26. Doghouse plots for a CL600 with OEI and deployed flaps were produced at low altitude. At 50 ft. ASL, the CL600 has a maximum net climb gradient of 5%. By the time the CL600 climbs to 1000 ft ASL, the maximum net climb gradient is reduced by 0.5%. The degradation due to altitude change is slight, but in the early stages of takeoff every bit of climb gradient matters. If the aircraft lifts off the ground at the optimal speed for climb performance, the climb performance is still at a maximum of nearly 5%. From 50 to 100 ft. ASL, the aircraft is restricted to a maximum bank angle of 15 degrees, per AC-120-91, limiting the initial turn performance. During this segment, the aircraft travels up to 1,000 ft. downrange. Upon reaching 100 ft. ASL, a tighter turn can be executed such that the turn radius is reduced to 11,000 ft., if the airspeed is at the optimal climb speed the aircraft can maintain a 4.5% climb gradient. As expected, climb performance declines as the aircraft gains altitude. Traveling in a straight flight path, the aircraft would travel an additional 2666 ft. downrange before being able to use its full turn performance.

At 500 ft. ASL, the aircraft can increase its bank to 25 degrees. At this maximum bank, the maximum net climb gradient is 4.5% with a resulting 8,500 ft. turn radius. The VFR map of Burbank airport[10] shows that a fully loaded CL600 can perform the Van Nuys SID.[11]

If the same takeoff procedure is performed by an Airbus a320, the results are less definitive. Upon takeoff, the a320 can only achieve approximately 2.5% climb gradient with OEI while fully loaded. It is important to note that this is just above the CFR required 2.4% climb gradient yielding a 4% margin of safety. Since Burbank is at an elevation of 778 ft., climb performance is diminished further thereby disqualifying the aircraft from operation due to a lack of climb performance. To increase climb performance the TOW weight must be reduced by at least 10,000

lbs. Even after weight reduction, the problem still exists since the optimal climbing airspeed for the a320 is around 170 knots TAS. At a TOW of 162,000 lbs travelling at 170 KTAS, this aircraft would cover 16,000 ft. before reaching an altitude of 500 ft completing a 90 degree heading change. The aircraft is operating in a space where it must travel fast to maintain climb performance, but in doing so hinders the aircrafts turning performance. This result shows that at high weight, this aircraft does pose a credible risk of failing to meet obstacle avoidance requirements. In an airport like Bob Hope Airport the operator must choose between climb performance or turn performance in a scenario where both are needed.

Furthermore, simplifications made in this simulation may degrade performance further. During the 1st segment of takeoff, the landing gear is extended which adds a large amount of drag. The duration of 1st segment is also variable due to the reaction time of a pilot and time required to stow the landing gears. This simulation also neglects the presence of head/tail wind. In the presence of a headwind, the aircraft will indicate a higher airspeed than its TAS. This may cause the pilot to operate the aircraft at a speed off the optimal climb speed. Also, the cue speeds of the aircraft directly impact the turn-climb performance. If cue speeds are arbitrarily defined off optimal climb speed, the aircraft is expected to maintain the selected speed until the end of the second segment of climb. This simulation assumes an ISA standard day. High temperatures further diminish performance. Lastly, bleed air settings reduce the thrust produced. The effects of temperature, pressure altitude, and anti-ice can increase the amount of bleed air nonlinearly and require table lookups to find the thrust degradation. The compounded effects of these factors can drastically change the behavior of an aircraft. They are also changing day to day making an overarching set of solutions unobtainable.

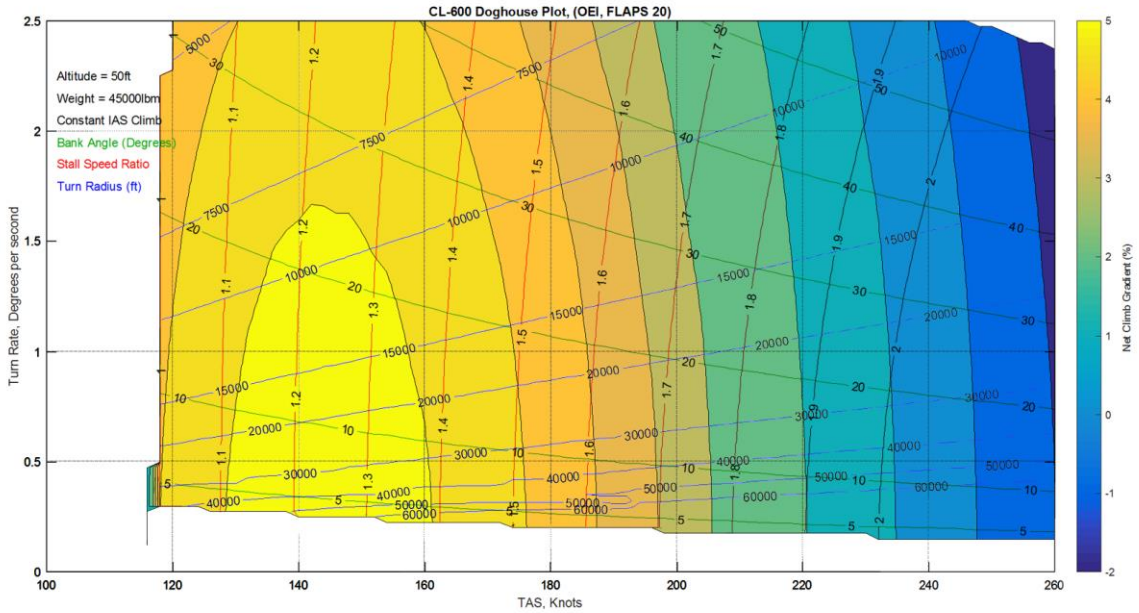

Figure 22. Bombardier CL600 Doghouse Plot at 50ft Altitude and 45,000lb Weight. *This Doghouse plot is part of a collection of Doghouse Plots that illustrate the effects of altitude on the turn-climb performance of a CL600.*

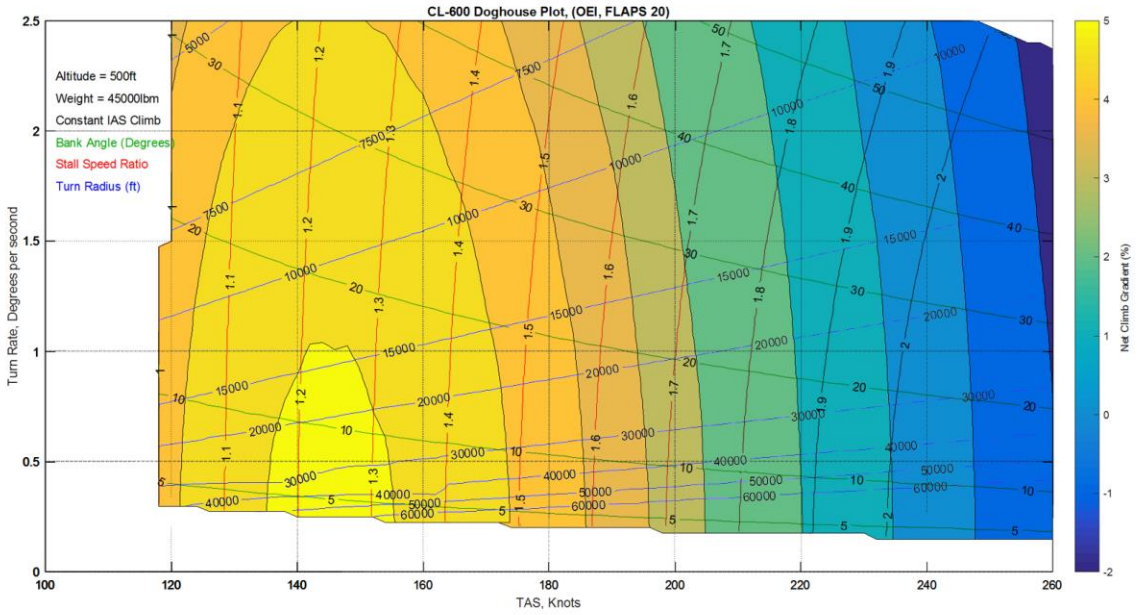

Figure 23. Bombardier CL600 Doghouse Plot at 500ft Altitude and 45,000lb Weight. *This Doghouse plot is part of a collection of Doghouse Plots that illustrate the effects of altitude on the turn-climb performance of a CL600.*

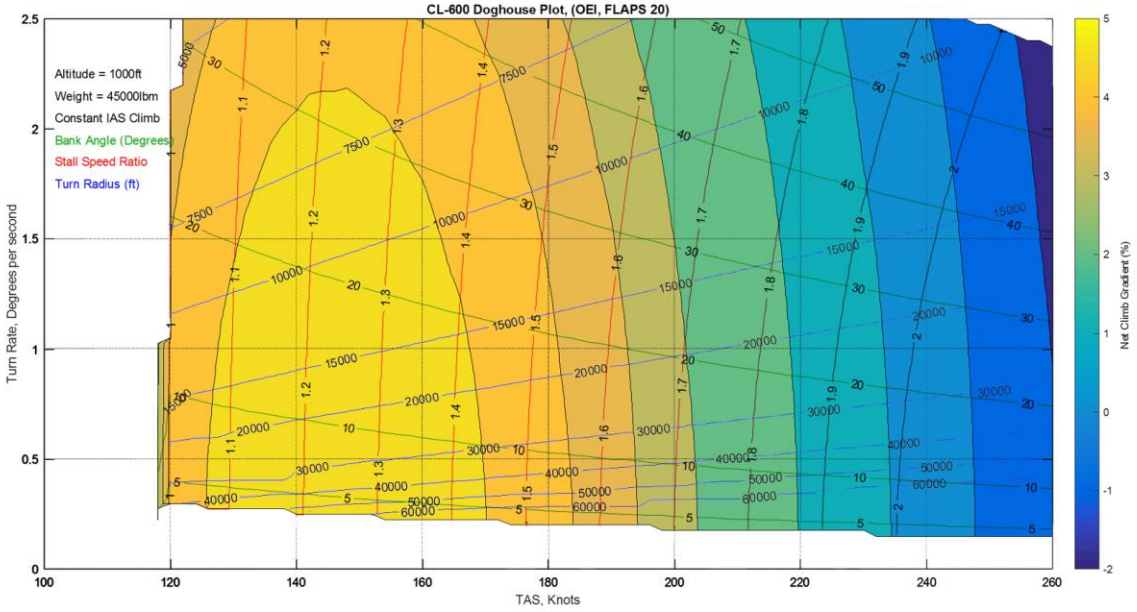

Figure 24. Bombardier CL600 Doghouse Plot at 1,000ft Altitude and 45,000lb Weight. *This Doghouse plot is part of a collection of Doghouse Plots that illustrate the effects of altitude on the turn-climb performance of a CL600.*

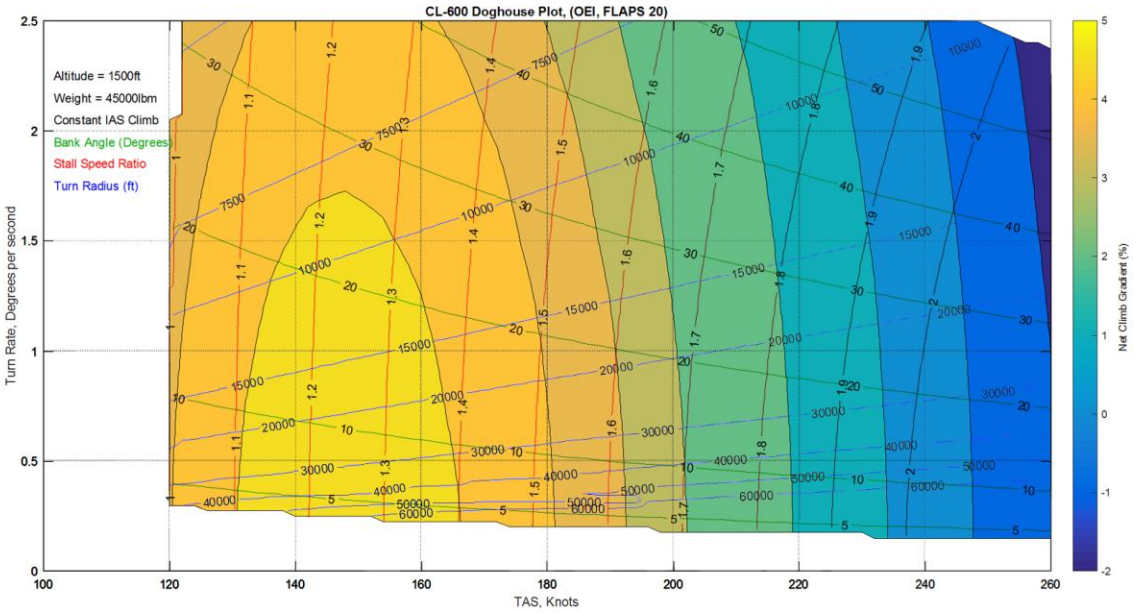

Figure 25. Bombardier CL600 Doghouse Plot at 1,500ft Altitude and 45,000lb Weight. *This Doghouse plot is part of a collection of Doghouse Plots that illustrate the effects of altitude on the turn-climb performance of a CL600.*

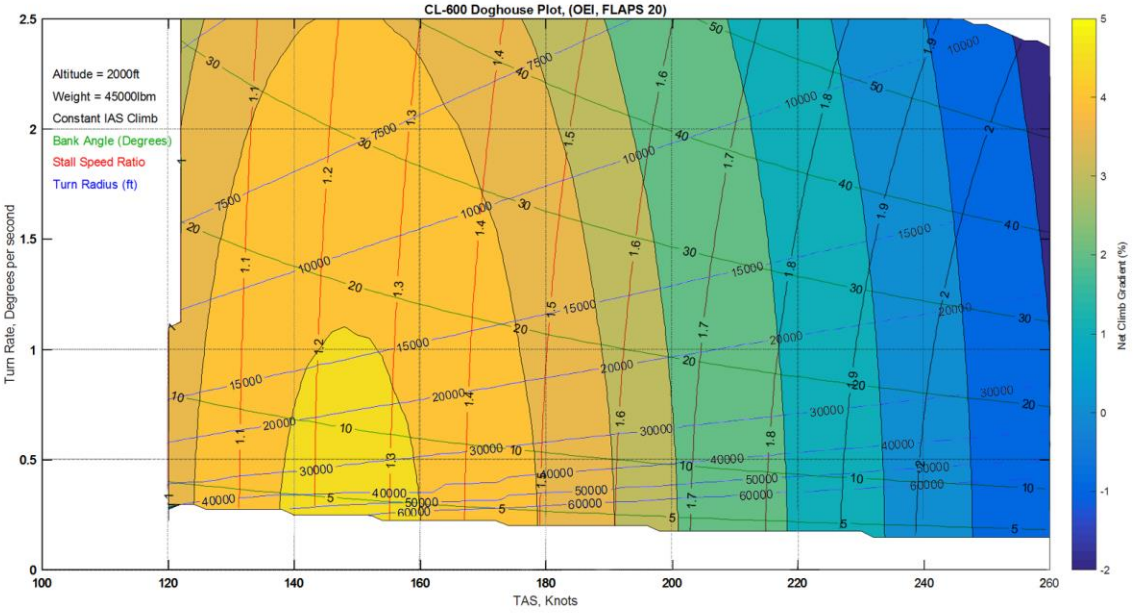

Figure 26. Bombardier CL600 Doghouse Plot at 2,000ft Altitude and 45,000lb Weight. *This Doghouse plot is part of a collection of Doghouse Plots that illustrate the effects of altitude on the turn-climb performance of a CL600.*

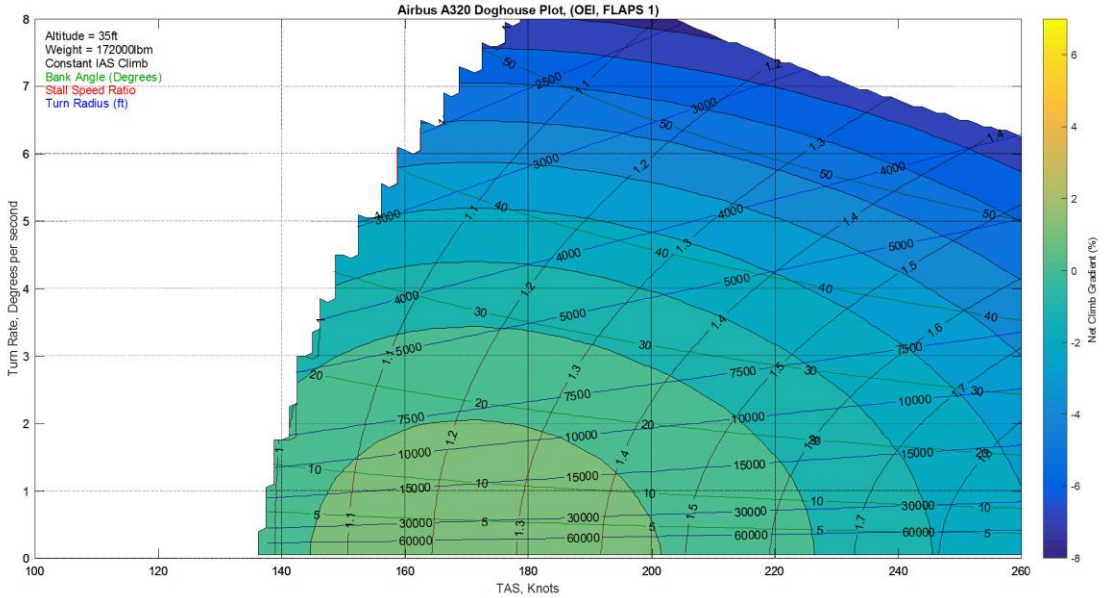

Figure 27. Airbus a320 Doghouse Plot at 35ft Altitude and 172,000lb Weight. *This Doghouse plot is part of a collection of Doghouse Plots that illustrate the effects of weight at takeoff on the turn-climb performance of an Airbus a320.*

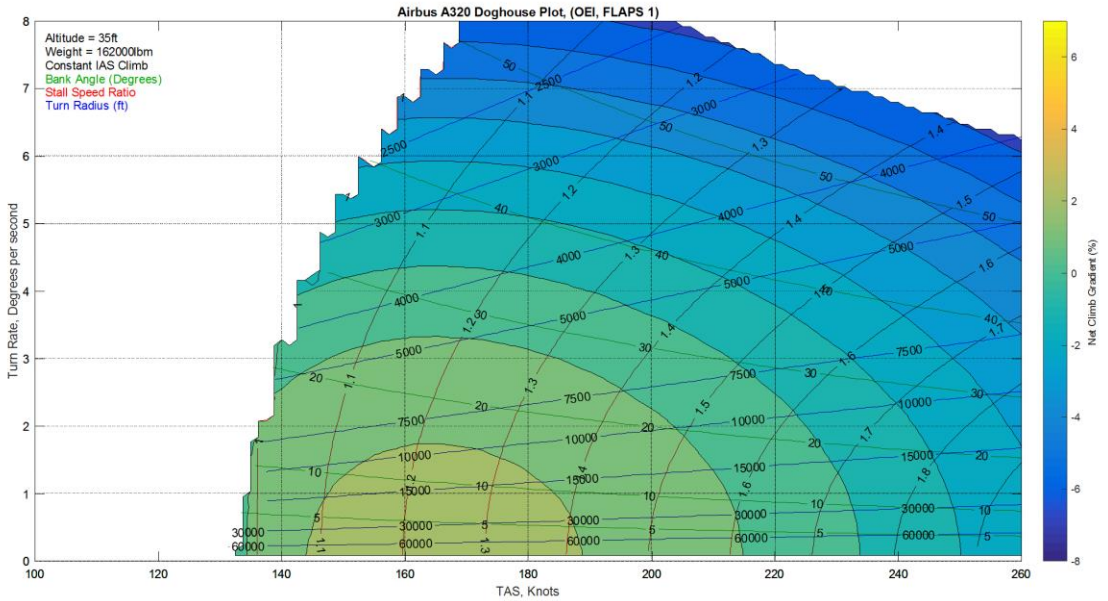

Figure 28. Airbus a320 Doghouse Plot at 35ft Altitude and 162,000lb Weight. *This Doghouse plot is part of a collection of Doghouse Plots that illustrate the effects of weight at takeoff on the turn-climb performance of an Airbus a320.*

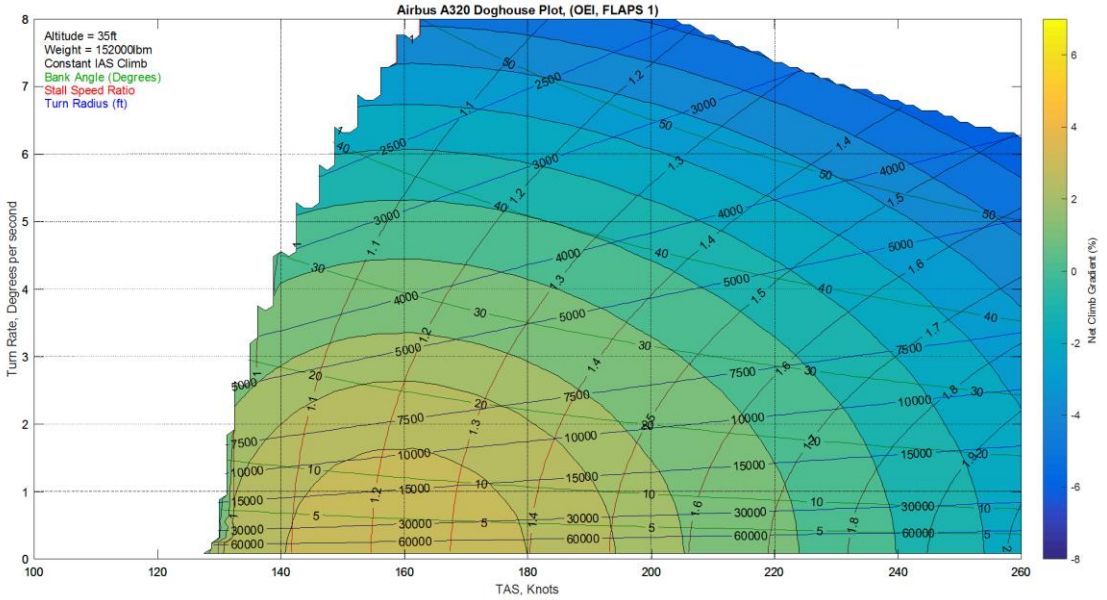

Figure 29. Airbus a320 Doghouse Plot at 35ft Altitude and 152,000lb Weight. *This Doghouse plot is part of a collection of Doghouse Plots that illustrate the effects of weight at takeoff on the turn-climb performance of an Airbus a320.*

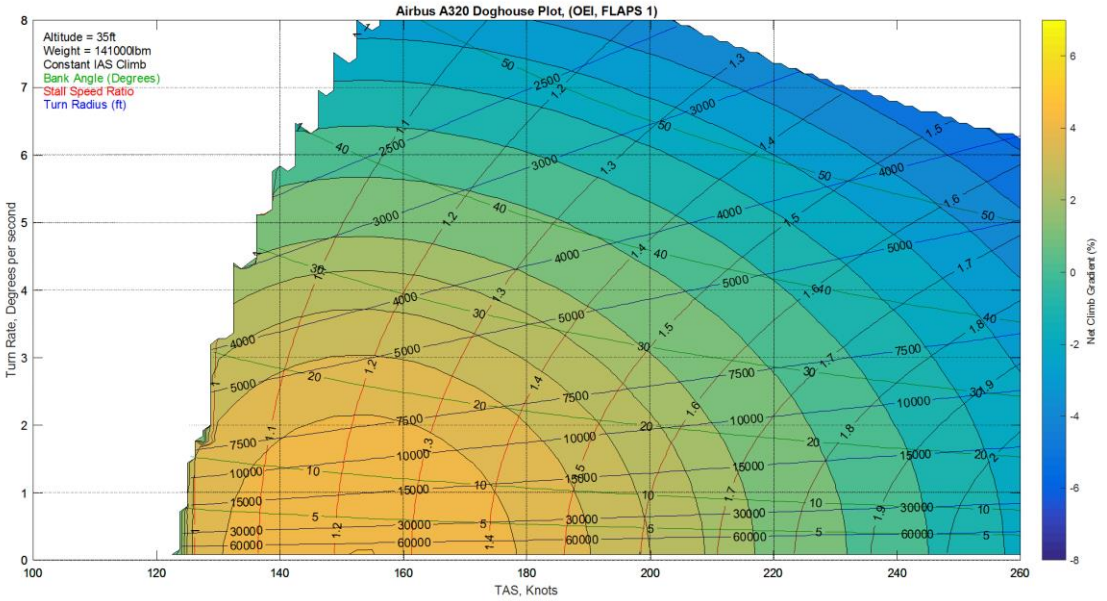

Figure 30. Airbus a320 Doghouse Plot at 35ft Altitude and 142,000lb Weight. *This Doghouse plot is part of a collection of Doghouse Plots that illustrate the effects of weight at takeoff on the turn-climb performance of an Airbus a320.*

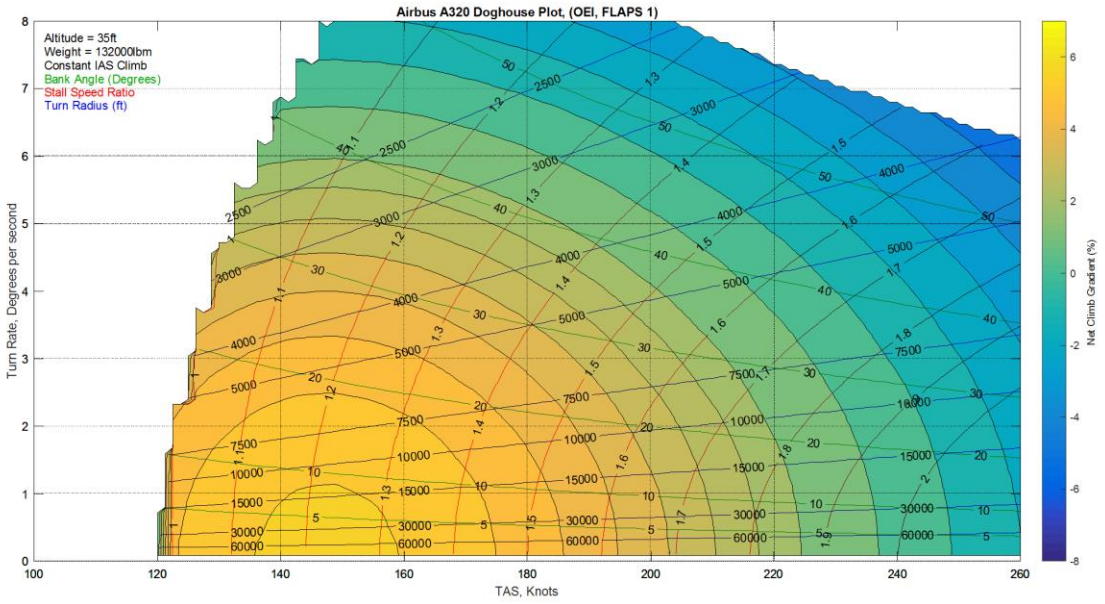

Figure 31. Airbus a320 Doghouse Plot at 35ft Altitude and 132,000lb Weight. *This Doghouse plot is part of a collection of Doghouse Plots that illustrate the effects of weight at takeoff on the turn-climb performance of an Airbus a320.*

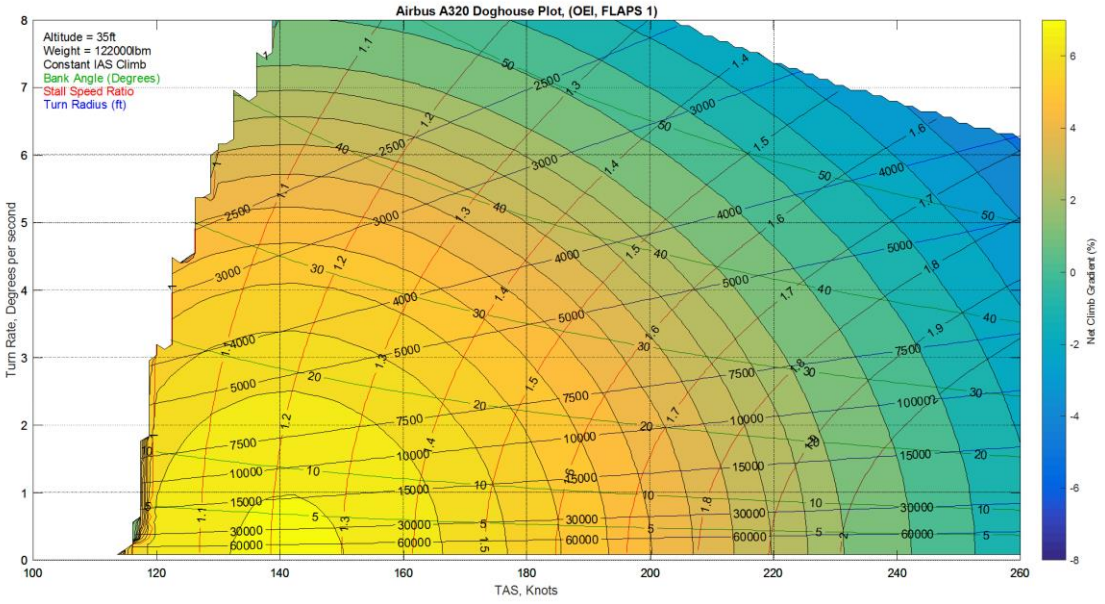

Figure 32. Airbus a320 Doghouse Plot at 35ft Altitude and 122,000lb Weight. *This Doghouse plot is part of a collection of Doghouse Plots that illustrate the effects of weight at takeoff on the turn-climb performance of an Airbus a320.*

VII. Conclusion

Energy-Manueverability Theory can be used to develop a straightforward process to formulate Doghouse plots for existing aircraft. Any aircraft can be "reverse engineered;" its performance modelled using publicly availabile aircraft geometry and propulsion information. Using the Doghouse plot, we can then assess the full turn-climb performance of an aircraft at any altitude, temperature, weight, or flap configuration.

The Doghouse plot adds insight to obstacle avoidance during takeoff, especially in one-engine-inoperative scenarios. Obstacle avoidance simulations can easily utilize the data provided by the Doghouse plot to accurately approximate the net takeoff path. These simulations can then be compared to the Standard Instrument Departures for given airports to assess the feasibility of a takeoff.

Airplane Flight Manuals examined in this study do not present clear representations of turn-climbs, nor give specific reference to the maneuver. Turn-climb performance is not explicitly required by the Code of Federal Regulations. Furthermore, the current regulatory landscape of obstacle avoidance was supplemented by AC-120-91 due to the overly restrictive limits on bank. The model presented in this study is credible for bank angles that are encompassed by the FAA and AC-120-91; however, I suggest that banking further than 25 degrees should be verified via flight simulators and test. A limitation of this study is the EDET and NPSS models. Both models are assembled by what can be found online. Proprietary performance data from manufacturers would greatly benefit this study and the models presented herein. Nevertheless, the Doghouse plot is valuable to provide a new understanding of aircraft performance.

References

[1] Coram, R., *Boyd: The Fighter Pilot Who Changed the Art of War*, Back Bay Books, New York, 2002, Chaps. 10, 15.

[2] Shaw, R., *Fighter Combat: Tactics and Maneuvering*, United States Naval Institute, Annapolis, 1985, pp. 337-417.

[3] Boyd, J. R., Christie, T. P., and Gibson J.E., "Energy-Maneuverability," APGD-TDR-64-28, Vol 1, March, 1966.

[4] 14 C.F.R. § 25.119, "Performance: Landing Climb". (2016).

[5] 14 C.F.R. § 25.121, "Performance: One engine-inoperative". (2016).

[6] 14 C.F.R. § 25.1585 "Airplane Flight Manual: Operating procedures". (2016).

[7] 14 C.F.R. § 121.189, "Airplanes: Turbine engine powered: Takeoff limitations". (2016).

[8] 14 C.F.R. § 135.379, "Large transport category airplanes: Turbine engine powered: Takeoff limitations". (2016).

[9] 14 C.F.R. § 25.123, "En route flight paths". (2016).

[10] "VFR – Digital Aeronautical Charts," Digital Aviation LLC, [online map] URL: http://www.vfrmap.com [cited 18 March 2017].

[11] "Van Nuys Three," *Bob Hope Airport*, AirNav LLC, [online PDF] URL: http://www.airnav.com/airport/KBUR [cited 8 April 2017].

[12] 14 C.F.R. § 25.1587, "Airplane Flight Manual: Performance information". (2016).

[13] 14 C.F.R. § 25.1581, "Airplane Flight Manual: General". (2016).

[14] 14 C.F.R. § 25.111, "Performance: Takeoff path". (2016).

[15] 14 C.F.R. § 25.115, "Performance: Takeoff flight path". (2016).

[16] 14 C.F.R. § 25.119, "Performance: Landing climb: All-engines-operating". (2016).

[17] 14 C.F.R. § 135.398, "Airplane Performance Operating Limitations: Commuter category airplanes performance operating limitations". (2016).

[18] 14 C.F.R. § 25.107, "Performance: Takeoff speeds". (2016).

[19] 14 C.F.R. § 25.125, "Performance: Landing". (2016).

[20] 14 C.F.R. § 25.149, "Controllability and Maneuverability: Minimum control speed". (2016).

[21] 14 C.F.R. § 25.335, "Flight Maneuver and Gust Conditions: Design airspeeds". (2016).

[22] Advisory Circular (AC) 23-19A, *Airframe Guide for Certification of Part 23 Airplanes*, United States Department of Transportation, Federal Aviation Administration (FAA), 30 April 2007.

[23] 14 C.F.R. § 91.117, "Flight Rules: Aircraft speed". (2016).

[24] Advisory Circular (AC) 25.1581-1, *Airplane Flight Manual*, United States Department of Transportation, Federal Aviation Administration (FAA), Change 1, 16 October 2012.

[25] Advisory Circular (AC) 120-91, *Airport Obstacle Analysis*, United States Department of Transportation, Federal Aviation Administration (FAA), 5 May 2012.

[26] Hawker 800XP AFM

[27] Cessna CL680 AFM

[28] BeechJet 400 AFM

[29] Boeing 737 FCOM, Performance Inflight, 737-500 CFM56-3_20K FAA, June 2011.

[30] Airbus Customer Services, *Getting to Grips with Aircraft Performance*, Airbus S.A.S., France, 2002, pp 70.

[31] Merritt, S. R., Cliff, E. M., and Kelley, H. J., "Energy-modelled Climb and Climb-dash – the Kaiser technique," *Automatica*, Vol. 21, No. 3, 1985, pp. 319-321.

[32] Takahashi, T.T. Aircraft Performance and Sizing: Vol. I and II, Momentum Press, New York (2016).

[33] Anon., "Jet Transport Performance Methods," Boeing D6-1420, 7th Edition, Boeing Corp., Seattle, WA, 1989.

[34] Feagin, R. C., and Morrison W. D., "Delta Method, An Empirical Drag Buildup Technique," NASA-CR-151971. Lockheed-California Co., Burbank, 1978.

[35] NPSS, Numerical Propulsion System Simulation, Software Package, Ver. 2.3.0.1, Ohio Aerospace Institute, Cleveland, OH, 2010.